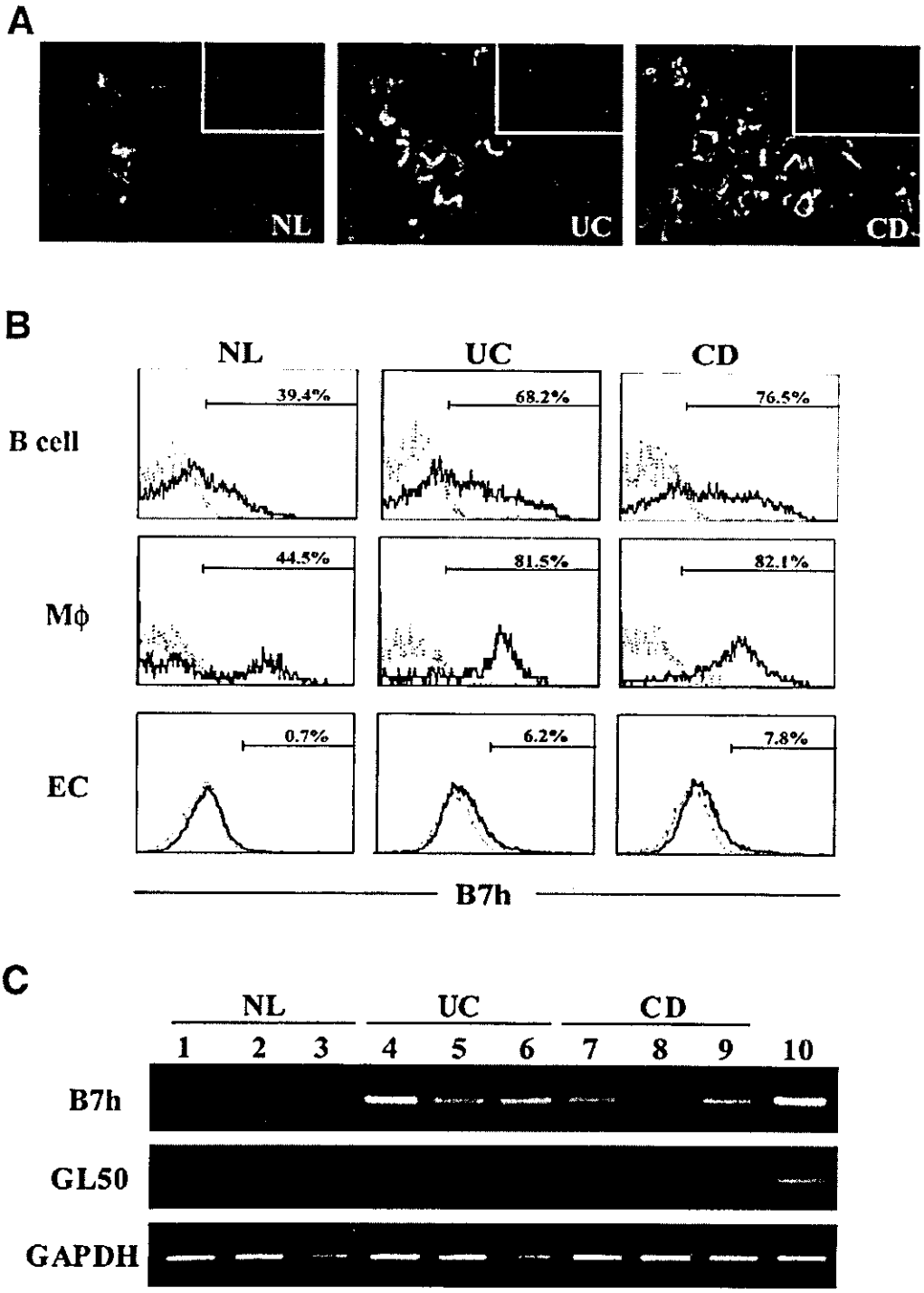

Figure 3. (*A*) Confocal imaging of mucosa from NL, UC, and CD stained with anti-B7h mAb. *Insets* show imaging stained by control IgG. (*B*) Expression of B7h protein on freshly isolated LP B cells, macrophages, and epithelial cells (EC) obtained from NL, UC, and CD (*thick line*; control staining is shown as *thin line*). B7h is down-regulated on LP B cells and LP macrophages from NL, but significantly up-regulated on those from UC and CD. B7h is slightly, but significantly, up-regulated on EC from both UC and CD, as compared with those from NL. (*C*) Transcripts of B7h and GL50 in EC obtained from NL (*lanes 1–3*), UC (*lanes 4–6*), and CD (*lanes 7–9*). As positive control for B7h and GL50, transcripts of LPMC obtained from NL (*lane 10*) are shown. As internal controls, transcripts of GAPDH mRNA are shown.

Cytokine Production

Finally, to address the disease-specific contribution of ICOS, we measured the amounts of IL-2, IFN-γ IL-10, IL-4, and IL-5 produced by PBMC and LPMC from the 3 groups after in vitro stimulation with anti-ICOS, anti-CD28, or control mAb in the presence or absence of anti-CD3. As previously reported, PBMC stimulated by anti-CD3/ICOS produced higher amounts of IL-10 and lower amounts of IL-2 as compared with anti-CD3/CD28. PBMC stimulated by anti-CD28 or anti-ICOS alone produced minimal amounts of cytokines as well as control IgG alone. There was no difference in cytokine amounts among the three groups (data not shown).

In LPMC, the patterns of cytokine secretion were mostly similar to those of PBMC (higher IL-10 production and lower IL-2 production). However, in contrast to PBMC, LPMC stimulated by anti-ICOS in the absence of

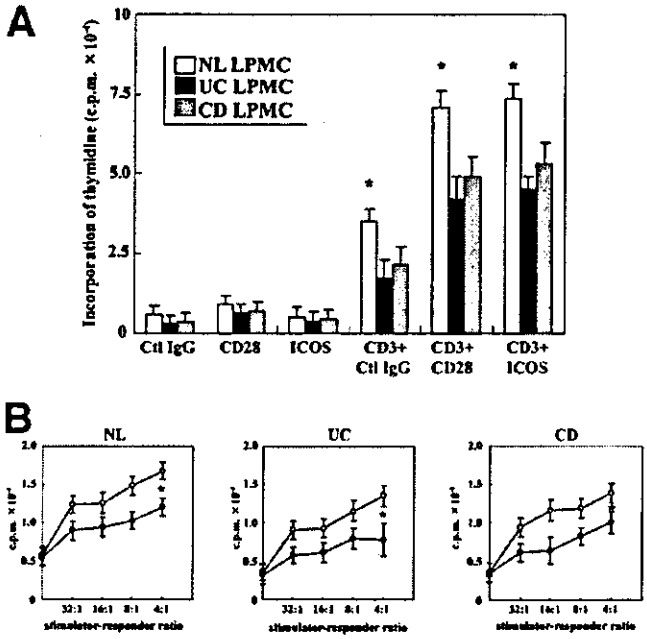

Figure 4. (*A*) Proliferative responses of LPMC obtained from NL (n = 5), CD (n = 5), and UC (n = 5) induced by plate-bound control IgG (10 μg/mL), anti-CD28 mAb (10 μg/mL), or anti-ICOS mAb (20 μg/mL) in the presence or absence of plate-bound anti-CD3 mAb (1 μg/mL). Proliferative activity was measured after 72-hour culture. *Error bars* represent SEM from studies of 5 experiments for NL, UC, and CD. ICOS costimulation is comparable with CD28 costimulation. The proliferative response of LPMC from patients with UC and CD is significantly lower than that from NL ($P < 0.05$). (*B*) Mixed lymphocyte reaction (MLR) assay between responder (LP $CD4^+$ T cells) and stimulator (allogenic peripheral blood monocytes) in the presence of control IgG (*open circle*) or anti-B7h mAb (*solid circle*). The responder proliferates in a dose-dependent manner, and the blockade of ICOS-B7h interaction inhibits MLR. There are no significant differences among the 3 groups (*$P < 0.05$).

anti-CD3 from all 3 groups secreted small but significantly higher amounts of IL-10 than anti-CD28 alone or control IgG alone. NL LPMC stimulated with anti-CD3 in the presence or absence of costimulation (anti-CD28 or anti-ICOS) secreted significantly higher amounts of IL-2, IL-4, and IL-10 but not IL-5 and IFN-γ when compared with those of UC and CD LPMC. IL-5 production by anti-ICOS alone or anti-CD3/ICOS from UC LPMC was significantly higher than that from CD or NL LPMC. In addition, IFN-γ production was significantly lower in UC LPMC as compared with CD or NL LPMC when stimulated with anti-CD3/ICOS. To further elucidate potential Th1 activity in CD, we measured IFN-γ production when stimulated with anti-CD3/ICOS in the presence of IL-12. As expected, anti-CD3/ICOS/IL-12-stimulated LPMC from CD produced significantly higher amounts of IFN-γ as compared with that from NL or UC. Similar results were obtained when LPMC were stimulated with anti-CD3/IL-12 or anti-CD3/anti-CD28/IL-12 (Figure 6).

Discussion

In this study, we have demonstrated for the first time that a novel costimulatory molecule, ICOS, was markedly up-regulated in LP $CD4^+$ T cells from patients with active but not inactive UC and CD. Furthermore, ICOS in LP $CD4^+$ T cells from acute colitis, such as infectious and ischemic colitis, was not increased regardless of the disease activity. In addition, we showed that ICOS was not increased in PB $CD4^+$ T cells in either NL or in patients with active or inactive IBD. Most importantly, we also demonstrated that anti-ICOS stimulation enhanced production of a Th2 cytokine, IL-5, in UC and production of a Th1 cytokine, IFN-γ, in CD. Our present results suggest that ICOS up-regulation is limited to the inflammatory sites of IBD and plays a major role in chronic intestinal inflammation.

Consistent with a previous study showing that anti-ICOS antibody could enhance T-cell proliferation

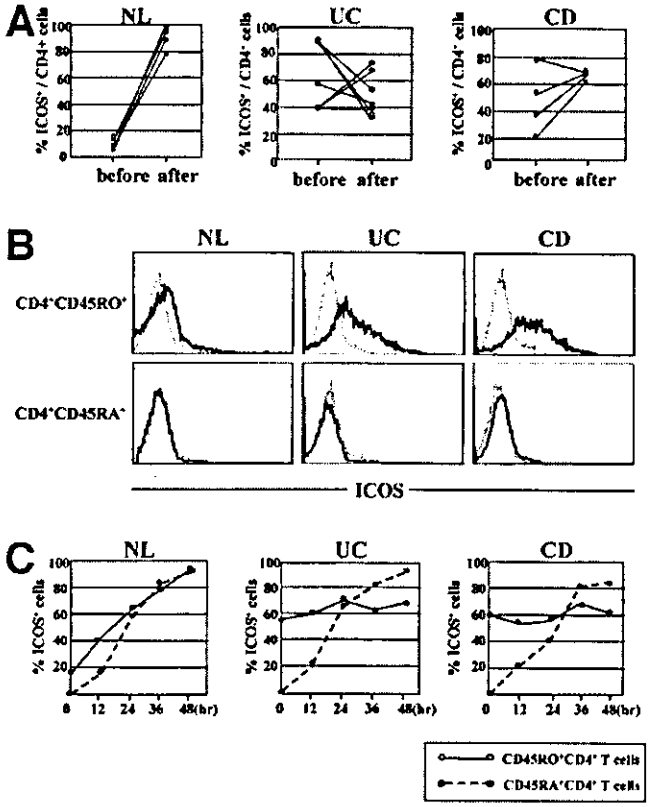

Figure 5. (*A*) Induction of ICOS on $CD4^+$ LPMC by anti-CD3 stimulation for 36 hours in vitro. LPMC from 3 groups were stimulated by plate-bound anti-CD3mAb, and the expression of ICOS was measured by flow cytometry using PE-anti-CD4 mAb and FITC-anti-ICOS mAb. (*B*) Expression of ICOS on naïve ($CD45RA^+$) or memory ($CD45RO^+$) LP T cells was measured using flow cytometry (*thick line*; control staining is shown as *thin line*). (*C*) Induction of ICOS on $CD4^+$ LP T cells was determined after separation of $CD45RA^+$ or $CD45RO^+$ T cells. ICOS expression is significantly up-regulated on $CD45RA^+$ T cells from all 3 groups and on CD45 RO^+ T cells from NL. Up-regulation of ICOS is dull on CD45 RO^+ T cells from UC and CD.

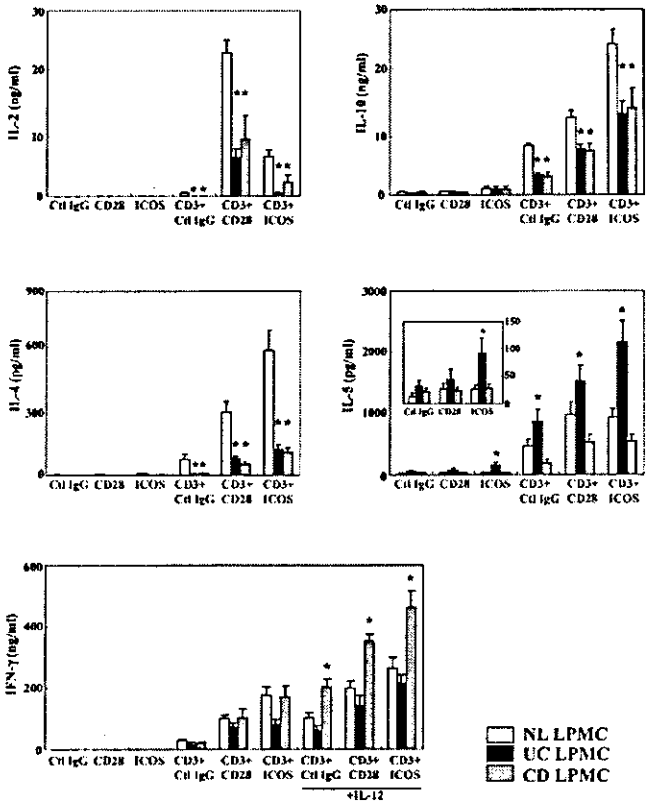

Figure 6. Cytokine productions of LPMC obtained from NL (n = 5), UC (n = 10), and CD (n = 10) induced by plate-bound control IgG (10 μg/mL), anti-CD28 mAb (10 μg/mL), or anti-ICOS mAb (20 μg/mL) in the presence or absence of plate-bound anti-CD3 mAb (1 μg/mL). In the study of IFN-γ, LPMC are also stimulated in the presence of IL-12 (10 ng/mL). *Error bars* represent SEM from studies of 5 experiments for NL and 10 experiments for UC and CD. *Inset* shows magnified figure of IL-5 productions stimulated by control IgG, anti-CD28, and anti-ICOS alone (*$P < 0.05$).

through TCR signal,[21] anti-CD3/ICOS stimulation enhanced LPMC proliferation comparable with anti-CD3/CD28 stimulation. However, NL LPMC proliferated more potently than IBD LPMC with anti-CD3 stimulation, with or without costimulation. This paradoxical result of LPMC proliferation via the CD3/CD28 pathway has already been observed by Fuss et al.[6] They concluded that LPMC from IBD patients were less responsive to anti-CD3 stimulation because of chronic exposure to inflammatory environments in the intestine as compared with NL LPMC. This is in line with a recent study showing that chronic inflammation down-regulates the T-cell receptor ζ chain and thereby induces resistance against anti-CD3 stimulation in T cells.[32] Although ICOS expression in NL LPMC was significantly lower than that of IBD LPMC, the proliferative responses of NL LPMC by anti-CD3/ICOS stimulation were much higher compared with those of IBD patients. To address the discrepancy, we next compared ICOS expression on LPMC before and after in vitro anti-CD3 stimulation. Although ICOS expression was rapidly induced and most $CD4^+$ T cells (>80%) expressed ICOS in NL, its expression level increased moderately (70%) in CD and decreased (50%) in UC after activation. Furthermore, we separately examined ICOS expression in $CD45RO^+$ (memory) and $CD45RA^+$ (naïve) subpopulations. Consistent with previous reports, $CD45RA^+$ $CD4^+$ LP cells did not express ICOS, whereas $CD45RO^+$ $CD4^+$ LP cells did, especially from UC or CD patients. Before anti-CD3 stimulation, ICOS expression on a $CD45RO^+$ subset was higher on UC or CD LP $CD4^+$ T cells than on NL LP $CD4^+$ T cells, which could be explained by the observation that memory cells were activated in IBD lamina propria. Intriguingly, whereas ICOS expression was remarkably enhanced in $CD45RO^+CD4^+$ NL LP cells when stimulated with anti-CD3, it remained at similar levels in the same population from UC or CD. This might be due to ICOS gene regulation specific to activated memory $CD4^+$ cells, or again due to the hyporesponsiveness of IBD LPMC to anti-CD3 antibody. Alternatively, it is also possible that ICOS is crucially involved in the early phase of $CD4^+CD45RA^+$ naïve T-cell activation rather than reactivation of $CD4^+CD45RO^+$ memory T cells. Therefore, total ICOS expression on NL LP $CD4^+$ cells could rapidly overtake that of IBD LP $CD4^+$ cells after CD3 stimulation, which in part explains their stronger proliferation with anti-ICOS costimulation than with IBD LP cells.

Initial studies have shown that ICOS-mediated costimulation was more effective than CD28 in the production of IL-10, and it also enhanced the production of other cytokines such as IL-4, IL-5, and IFN-γ with 50%–70% of the levels achieved with CD28.[21] Coyle et al. reported that Th2 cells express higher amounts of ICOS mRNA and protein[23] and Gonzalo et al. demonstrated that ICOS is critical for the Th2 lung mucosal injury model.[24] However, other studies have recently shown that ICOS blockade was effective for the Th1-mediated disease, EAE,[33] and cardiac allograft rejection.[34] To clarify the cytokine profile induced by anti-ICOS stimulation in IBD, we stimulated LPMC under various kinds of stimulating conditions. Fuss et al. previously reported that CD LP T cells produced increased IFN-γ production via the CD2/CD28 pathway compared with NL LP T cells, whereas IL-5 secretion was increased in UC LP T cells even without in vitro stimulation.[6] Consistent with this, we found that UC LPMC produced significantly increased amounts of IL-5 as compared with NL or CD LPMC when stimulated with anti-ICOS antibody alone or anti-CD3/ICOS. However, IL-4 and IL-10, 2 other Th2 cytokines, were secreted most promi-

nently from NL LPMC in any stimulatory condition tested in this study as Fuss et al.[6] demonstrated with similar data about IL-4. It remains to be clarified why UC LPMC enhance IL-5 but not IL-4, despite both cytokines being located in close proximity on human chromosome 5 and regulated by similar transcription factors.[35] Next, we examined Th1 cytokine production in CD LPMC. When LPMC were stimulated via CD3, costimulation with either anti-CD28 or anti-ICOS enhanced IFN-γ production from LPMC in all groups. However, we could not detect any differences between the NL and CD LPMC. Fuss et al. demonstrated similar data and implied the involvement of hyporesponsiveness to anti-CD3.[6] Again, chronic inflammation and exposure to intestinal antigen may confer resistance against anti-CD3 stimulation and thereby modify cytokine production. In particular, the T-cell receptor ζ chain was down-regulated by chronic inflammation in the setting of a Th1 but not a Th2 response.[32] Based on these findings, we added IL-12 to the anti-CD3/CD28 or ICOS stimulatory system to emphasize the microenvironment in CD because IL-12 augments IFN-γ production and has been shown to be increased in the lamina propria of CD patients.[36] In this condition, anti-ICOS, as well as anti-CD28, increased IFN-γ production in both groups, but the costimulatory effect was more effective in CD LPMC. Thus, IL-12 has a dispensable role on CD LPMC to augment the Th1 response, and anti-ICOS costimulation synergistically enhanced IL-12 stimulation. As discussed previously, the association of ICOS costimulation and the T-cell cytokine pattern is still a matter of debate. First, we could not detect any differences of ICOS expression between UC (Th2-like disease) and CD (Th1-mediated disease). Second, anti-ICOS antibody enhanced the secretion of all cytokines tested, irrespective of Th1 or Th2, from anti-CD3 stimulated LPMC. These data suggest that the ICOS signal is neither restricted to Th1 nor Th2 responses, at least in the lamina propria.

To further reinforce the possibility of the contribution of ICOS to the pathogenesis of IBD, we examined the expression of the ICOS ligand B7h in intestinal mucosa. Flow cytometry and immunohistochemistry revealed significantly increased expression of B7h on B cells and macrophages in the inflamed mucosa. Its expression was also very faintly detected on epithelial cells from IBD patients. The distribution suggests that the interaction between T cells and professional APC via the ICOS/B7h system plays an important role in chronic intestinal inflammation.

Recently Akbari et al. showed that regulatory T cells inhibit inflammation through ICOS-B7h engagement.[31] In their study, when naïve T cells interacted with IL-10-producing dendritic cells, they differentiated into ICOS-expressing memory T cells and produced significant amounts of IL-10 but no IL-4 and IFN-γ through ICOS-B7h interaction. It has also been reported that $ICOS^+$ T cells could be divided into 3 fractions by their cytokine production pattern: $IL\text{-}10^{high}/IL\text{-}4^{low}/IFN\text{-}\gamma^{low}$, $IL\text{-}10^{high}/IL\text{-}4^{high}/IFN\text{-}g^{low}$, and $IL\text{-}10^{high}/IL\text{-}4^{low}/IFN\text{-}g^{high}$ fraction.[37] In contrast to ICOS-expressing regulatory T cells predominantly producing IL-10, LPMC stimulated by anti-ICOS produced not only IL-10 but also IL-4 and IFN-γ. In addition, the proliferation of LPMC was enhanced by anti-ICOS costimulation and was inhibited by blockade of the ICOS-B7h interaction. Furthermore, we demonstrated the ameliorating effect of an anti-ICOS monoclonal antibody in a murine model of chronic colitis.[38] Taken together, IL-10 production from anti-ICOS stimulated LPMC may function in a counter-regulatory role rather than an active regulatory one; however, there may be a small fraction of ICOS-expressing regulatory T cells. Further studies will be needed to address this issue.

In conclusion, ICOS and B7h are highly expressed in inflamed mucosa and are involved in a distinct cytokine production of LPMC in UC and CD; thus, ICOS might be an ideal therapeutic target without systemic immunosuppression because its expression is exclusively limited to activated $CD4^+$ LPMC in inflammatory sites.

References

1. Strober W, Neurath MF. Immunological diseases of the gastrointestinal tract. In: Rich RR, ed. Clinical Immunology. St. Louis: Mosby, 1996:1401–1428.
2. MacDonald TT, Monteleone G. IL-12 and Th1 immune responses in human Peyer's patches. Trends Immunol 2001;22:244–247.
3. Sartor RB. Role of the intestinal micro flora in pathogenesis and complications. In: Scolmerich JH, Goebell W, Kruis W, Hohenberger W, eds. Inflammatory bowel diseases: pathophysiology as basis of treatment. London: Kluwer Academic, 1992:175–187.
4. Schreiber S. Inflammatory bowel disease: immunologic concepts. Hepatogastroenterology 2000;47:15–28.
5. MacDonald TT, Monteleone G, Pender LF. Recent developments in the immunology of inflammatory bowel disease. Scand J Immunol 2000;51:2–9.
6. Fuss IJ, Neurath M, Boirivant M, Klein JS, de la Motte C, Strong SA, Fiocchi C, Strober W. Disparate $CD4^+$ lamina propria (LP) lymphokine secretion profiles in inflammatory bowel disease. Crohn's disease LP cells manifest increased secretion of IFN-γ, whereas ulcerative colitis LP cells manifest increased secretion of IL-5. J Immunol 1996;157:1261–1270.
7. Kanai T, Watanabe M, Okazawa A, Nakamaru K, Okamoto M, Naganuma M, Ishii H, Ikeda M, Kurimoto M, Hibi T. Interleukin 18 is a potent proliferative factor for intestinal mucosal lymphocytes in Crohn's disease. Gastroenterology 2000;119:1514–1523.
8. Kanai T, Watanabe M, Okazawa A, Sato T, Yamazaki M, Okamoto S, Ishii H, Totsuka T, Iiyama R, Okamoto R, Ikeda M, Kurimoto M, Takeda K, Akira S, Hibi T. Macrophage-derived IL-18-mediated intestinal inflammation in the murine model of Crohn's disease. Gastroenterology 2001;121:875–888.

9. Bretscher PA. A two-step, two-signal model for the primary activation of precursor helper T cells. Proc Natl Acad Sci U S A 1999;96:185–190.
10. Bromley SK, Iaboni A, Davis SJ, Whitty A, Green JM, Shaw AS, Weiss A, Dustin ML. The immunological synapse and CD28-CD80 interactions. Nat Immunol 2001;2:1159–1166.
11. Lonschow DJ, Walunas TL, Bluestone JA. CD28/B7 system of T cell costimulation. Ann Rev Immunol 1996;14:233–258.
12. Linsley PS, Clark EA, Ledbetter JA. T cell antigen CD28 mediates adhesion with B cells by interacting with activation antigen B7/BB-1. Proc Natl Acad Sci U S A 1990;87:5031–5035.
13. Azuma M, Ito D, Yagita H, Okumura K, Phillips JH, Lanier LL, Somoza C. B70 antigen is a second ligand for CTLA4 and CD28. Nature 1993;366:76–79.
14. Perrin PJ, June CH, Maldonado JH, Ratts RB, Racke MK. Blockade of CD28 during in vitro activation of encephalitogenic T cells or after disease onset ameliorates experimental autoimmune encephalomyelitis. J Immunol 1999;163:1704–1710.
15. Tada Y, Nagasawa K, Ho A, Morito F, Ushiyama O, Suzuki N, Ohta H, Mak TW. CD28-deficient mice are highly resistant to collagen-induced arthritis. J Immunol 1999;162:203–208.
16. Mathur M, Herrmann K, Qin Y, Gulmen F, Li X, Krimins R, Weinstock J, Elliott D, Bluestone JA, Padrid P. CD28 interaction with either CD80 or CD86 are sufficient to induce allergic airway inflammation in mice. Am J Respir Cell Mol Biol 1999;21:498–509.
17. Liu Z, Geboes K, Hellings P, Maerten P, Heremans H, Vandenberghe P, Boon L, van Kooten P, Rutgeerts P, Ceuppens JL. B7 interactions with CD28 and CTLA4 control tolerance or induction of mucosal inflammation in chronic experimental colitis. J Immunol 2001;167:1830–1838.
18. Brunet JF, Denizot F, Luciani MF, Roux-Dosseto M, Suzan M, Mattei MG, Golstein P. A new member of the immunoglobulin superfamily CTLA-4. Nature 1987;328:267–270.
19. Linsley PS, Brady W, Urnes M, Grosmaire LS, Damle NK, Ledbetter JA. CTLA-4 is a second receptor for the B cell activation antigen B7. J Exp Med 1991;174:561–569.
20. Sharpe AH, Freeman GJ. The B7-CD28 superfamily. Nat Rev Immunol 2002;2:116–126.
21. Hutloff A, Dittrich AM, Beier KC, Eljaschewitsch B, Kraft R, Anagnostopoulos I, Kroczek RA. ICOS is an inducible T-cell co-stimulator structurally and functionally related to CD28. Nature 1999;397:263–266.
22. Tamatani T, Tezuka K, Hanzawa-Higuchi N. AILIM/ICOS: a novel lymphocyte adhesion molecule. Int Immunol 2000;12:51–55.
23. Coyle AJ, Lehar S, Lloyd C, Tian J, Delaney T, Manning S, Nguyen T, Burwell T, Schneider H, Gonzalo JA, Gosselin M, Owen LR, Rudd CE, Gutierrez-Ramos JC. The CD28-related molecule ICOS is required for effective T cell-dependent immune responses. Immunity 2000;13:95–105.
24. Gonzalo JA, Tian J, Delaney T, Corcoran J, Rottman JB, Lora J, Al-garawi A, Kroczek R, Gutierrez-Ramos JC, Coyle AJ. ICOS is critical for T helper cell-mediated lung mucosal inflammatory responses. Nat Immunol 2001;2:597–604.
25. Swallow MM, Wallin JJ, Sha WC. B7h, a novel costimulatory homolog of B7.1 and B7.2, is induced by TNFα. Immunity 1999;11:423–432.
26. Aicher A, Hayden-Ledbetter M, Brady WA, Pezzutto A, Richter G, Magaletti D, Buckwalter S, Ledbetter JA, Clark EA. Characterization of human inducible costimulator ligand expression and function. J Immunol 2001;164:4689–4696.
27. Yoshinaga SK, Whoriskey JS, Khare SD, Sarmiento U, Guo J, Horan T, Shih G, Zhang M, Coccia MA, Kohno T, Tafuri-Bladt A, Brankow D, Campbell P, Chang D, Chiu L, Dai T, Duncan G, Elliott GS, Hui A, McCabe SM, Scully S, Shahinian A, Shaklee CL, Van G, Mak TW. T-cell co-stimulation through B7RP-1 and ICOS. Nature 1999;402:827–832.
28. Brodie D, Collins AV, Iaboni A, Fennelly JA, Sparks LM, Xu XN, van der Merwe PA, Davis SJ. LICOS, a primordial costimulatory ligand? Curr Biol 2000;10:333–336.
29. Wang S, Zhu G, Chapoval AI, Dong H, Tamada K, Ni J, Chen L. Costimulation of T cells by B7-H2, a B7-like molecule that binds ICOS. Blood 2000;96:2808–2813.
30. Ling V, Wu PW, Miyashiro JS, Marusic S, Finnerty HF, Collins M. Differential expression of inducible costimulator-ligand splice variants: lymphoid regulation of mouse GL50-B and human GL50 molecules. J Immunol 2001;166:7300–7308.
31. Akbari O, Freeman GJ, Meyer EH, Greenfield EA, Chang TT, Sharpe AH, Berry G, DeKruyff RH, Umetsu DT. Antigen-specific regulatory T cells develop via the ICOS-ICOS-ligand pathway and inhibit allergen-induced airway hyperreactivity. Nat Med 2002;8:1024–1032.
32. Bronstein-Sitton N, Cohen-Daniel L, Vaknin I, Ezernitchi AV, Leshem B, Halabi A, Houri-Hadad Y, Greenbaum E, Zakay-Rones Z, Shapira L, Baniyash M. Sustained exposure to bacterial antigen induces interferon-γ-dependent T cell receptor ζ down-regulation and impaired T cell function. Nat Immunol 2003;4:957–964.
33. Rottman JB, Smith T, Tonra JR, Ganley K, Bloom T, Silva R, Pierce B, Gutierrez-Ramos JC, Ozkaynak E, Coyle AJ. The costimulatory molecule ICOS plays an important role in the immunopathogenesis of EAE. Nat Immunol 2001;2:605–611.
34. Ozkaynak E, Gao W, Shemmeri N, Wang C, Gutierrez-Ramos JC, Amaral J, Qin S, Rottman JB, Coyle AJ, Hancock WW. Importance of ICOS-costimulation in acute and chronic allograft rejection. Nat Immunol 2001;2:591–596.
35. Murphy KM, Reiner SL. The lineage decisions of helper T cells. Nat Rev Immunol 2002;2:933–944.
36. Monteleone G, Biancone L, Marasco R, Morrone G, Marasco O, Luzza F, Pallone F. Interleukin 12 is expressed and actively released by Crohn's disease intestinal lamina propria mononuclear cells. Gastroenterology 1997;112:1169–1178.
37. Lohning M, Hutloff A, Kallinich T, Mages HW, Bonhagen K, Radbruch A, Hamelmann E, Kroczek RA. Expression of ICOS in vivo defines $CD4^+$ effector T cells with high inflammatory potential and a strong bias for secretion of interleukin 10. J Exp Med 2003;197:181–193.
38. Totsuka T, Kanai T, Iiyama R, Uraushihara K, Yamazaki M, Okamoto R, Hibi T, Tezuka K, Azuma M, Akiba H, Yagita H, Okumura K, Watanabe M. Ameliorating effect of anti-inducible costimulator monoclonal antibody in a murine model of chronic colitis. Gastroenterology 2003;124:410–421.

Received August 15, 2002. Accepted December 11, 2003.

Address requests for reprints to: Toshifumi Hibi, M.D., Department of Internal Medicine, School of Medicine, Keio University, 35 Shinanomachi, Shinjuku-ku, Tokyo 160-8582, Japan. e-mail: thibi@sc.itc.keio.ac.jp; fax: (81) 3-3357-6156.

Supported in part by grants-in-aid from the Japanese Ministry of Education, Culture and Science; the Japanese Ministry of Health and Welfare; Chiyoda Mutual Life Foundation; and Japan Health Sciences Foundation.

The authors thank Drs. Miyuki Azuma, Katsunari Tezuka, and Hideo Yagita for critical comments and Drs. Masaki Kitajima, Masahiko Watanabe, Hirotoshi Hasegawa, and Akira Sugita for providing specimens.

T.S. and T.K. contributed equally to this work.

Ectopic CD40 Ligand Expression on B Cells Triggers Intestinal Inflammation[1]

Takahiro Kawamura,[2]* Takanori Kanai,[2]* Taeko Dohi,[‡] Koji Uraushihara,* Teruji Totsuka,* Ryoichi Iiyama,* Chikara Taneda,* Motomi Yamazaki,* Tetsuya Nakamura,* Tetsuya Higuchi,[†] Yuichi Aiba,[†] Takeshi Tsubata,[†] and Mamoru Watanabe[3]*

Several studies indicate that CD4$^+$ T cells, macrophages, and dendritic cells initially mediate intestinal inflammation in murine models of human inflammatory bowel disease. However, the initial role of B cells in the development of intestinal inflammation remains unclear. In this study we present evidence that B cells can trigger intestinal inflammation using transgenic (Tg) mice expressing CD40 ligand (CD40L) ectopically on B cells (CD40L/B Tg). We demonstrated that CD40L/B Tg mice spontaneously developed severe transmural intestinal inflammation in both colon and ileum at 8–15 wk of age. In contrast, CD40L/B Tg×CD40$^{-/-}$ double-mutant mice did not develop colitis, indicating the direct involvement of CD40-CD40L interaction in the development of intestinal inflammation. The inflammatory infiltrates consisted predominantly of massive aggregated, IgM-positive B cells. These mice were also characterized by the presence of anti-colon autoantibodies and elevated IFN-γ production. Furthermore, although mice transferred with CD4$^+$ T cells alone or with both CD4$^+$ T and B220$^+$ B cells, but not B220$^+$ cells alone, from diseased CD40L/B Tg mice, develop colitis, mice transferred with B220$^+$ B cells from diseased CD40L/B Tg mice and CD4$^+$ T cells from wild-type mice also develop colitis, indicating that the Tg B cells should be a trigger for this colitis model, whereas T cells are involved as effectors. As it has been demonstrated that CD40L is ectopically expressed on B cells in some autoimmune diseases, the present study suggests the possible contribution of B cells in triggering intestinal inflammation in human inflammatory bowel disease. *The Journal of Immunology,* **2004, 172: 6388–6397.**

Crohn's disease (CD)[4] and ulcerative colitis (UC) are the two major forms of chronic inflammatory bowel disease (IBD). Although their etiopathology remains unknown, increasing evidence has shown that an immune mechanism plays an important role in their pathogenesis (1–3). These include increased T cell infiltrates into gut, the production of cytokines by lamina propria (LP) T cells, and remission after treatment with immunosuppressants or by targeting proinflammatory cytokines. Although many animal experimental models clinically mimicking human IBD have been established, all these models induce diseases characterized by the common features of T cell- or macrophage/dendritic cell-dependent immune responses (4, 5).

One particular molecule that may be a potent target for the treatment of IBD is CD40 ligand (CD40L; CD154). This is found predominantly on activated CD4$^+$ T cells and interacts with CD40, which is expressed on B cells, APCs, and endothelial cells (6–8). In patients with IBD, increased numbers of T cells expressing CD40L have been detected in the LP, and these contribute to induce proinflammatory cytokines, including IL-12, by macrophages/dendritic cells (9, 10). Furthermore, it is known that mice with overexpressed CD40L on T cells develop chronic colitis with the infiltration of CD40L$^+$ T cells and CD40$^+$ cells into disease tissues (11). In both 2,4,6-trinitrobenzene sulfonic acid (TNBS)-induced (12) and SCID-transferred colitis models (13, 14), neutralizing anti-CD40L Abs prevent colitis. These data suggest that CD40/CD40L interactions are probably relevant in the development of colitis in humans and mice.

In contrast, CD40-expressing B cells, which interact with CD40L-expressing T cells, are able to promote the proliferation and survival of B cells, Ig isotype switching, and germinal center reaction (7, 15, 16). B cells possess a variety of immune functions, including the production of Igs and various cytokines, the presentation of Ags, and the regulation of dendritic cell function. Interestingly, functionally distinct roles of B cells have been reported in autoimmune diseases such as systemic lupus erythematosus (SLE) (17). B cells drive the development of several autoimmune disorders through the production of pathogenic autoantibodies. Similarly, circulating autoantibodies to colon epithelial cells have been consistently identified in patients with UC or CD by many investigators in reports that span at least 2 decades (18–20). Interestingly, accumulating evidence suggests that CD40L is ectopically expressed on B cells in the same range of their T cells in patients with SLE, although the pathogenic role of CD40L on B cells in SLE is unknown (21). At present, however, to our knowledge,

*Department of Gastroenterology and Hepatology, Graduate School, and [†]Department of Immunology, Medical Research Institute, Tokyo Medical and Dental University, Tokyo, Japan; and [‡]Department of Gastroenterology, Research Institute, International Medical Center of Japan, Tokyo, Japan

Received for publication June 25, 2003. Accepted for publication March 4, 2004.

The costs of publication of this article were defrayed in part by the payment of page charges. This article must therefore be hereby marked *advertisement* in accordance with 18 U.S.C. Section 1734 solely to indicate this fact.

[1] This work was supported in part by grants-in-aid for Scientific Research, Scientific Research on Priority Areas, Exploratory Research, and Creative Scientific Research from the Japanese Ministry of Education, Culture, Sports, Science, and Technology; the Japanese Ministry of Health, Labor, and Welfare; the Japan Medical Association; Foundation for Advancement of International Science; Terumo Life Science Foundation; Ohyama Health Foundation; Yakult Bio-Science Foundation; and Research Fond of Mitsukoshi Health and Welfare Foundation.

[2] T. Kawamura and T. Kanai contributed equally to this work.

[3] Address correspondence and reprint requests to Dr. Mamoru Watanabe, Department of Gastroenterology and Hepatology, Tokyo Medical and Dental University, Graduate School, 1-5-45 Yushima, Bunkyo-ku, Tokyo 113-8519, Japan. E-mail address: mamoru.gast@tmd.ac.jp

[4] Abbreviations used in this paper: CD, Crohn's disease; IBD, inflammatory bowel disease; LP, lamina propria; LPMC, lamina propria mononuclear cell; UC, ulcerative colitis; SLE, systemic lupus erythematosus; Tg, transgenic; TNBS, 2,4,6-trinitrobenzene sulfonic acid; TRITC, tetramethylrhodamine; WT, wild type.

0022-1767/04/$02.00

there have been no reports describing the expression of CD40L on B cells in patients with IBD.

Based on the fact that CD40L can be inducible on B cells in some autoimmune disorders and also several reports that described the association between IBD and SLE (22, 23), we investigated the possibility that intestinal inflammation may be induced by the primarily dysregulated B cells. To this end, we used transgenic (Tg) mouse lines expressing CD40L ectopically on B cells (CD40L/B Tg) (24). At 8–12 wk of age, CD40L/B Tg mice show increased number of B cells in spleen and increased serum IgG and IgM concentrations by ~4- and ~5-fold, respectively. In addition, B cells in CD40L/B Tg mice are resistant to apoptosis induced in vitro, probably due to constitutive CD40 signaling in B cells via CD40 (our unpublished observations). Interestingly, these mice developed SLE-like autoimmune disease, probably due to the production of many kinds of autoantibodies, such as anti-DNA Abs (24).

Surprisingly, we found that CD40L/B Tg mice developed severe transmural intestinal inflammations. Remarkably, the inflammatory infiltrates consisted predominantly of B cells. Although T cells also infiltrated inflamed lesions, they did so to a much lesser degree than B cells, and the CD4/CD8 ratio of LP T cells was decreased compared with that in control mice. Furthermore, we demonstrated that mice transferred with $CD4^+$ T cells alone or with both $CD4^+$ T and $B220^+$ B cells, but not $B220^+$ cells alone from diseased CD40L/B Tg mice, develop colitis similar to the original disease, indicating that the final cause of colitis is dysregulated $CD4^+$ T cells. However, we demonstrated that mice transferred with $B220^+$ B cells from diseased CD40L/B Tg mice and $CD4^+$ T cells from wild-type (WT) mice also developed colitis, albeit to a lesser extent than those transferred with $CD4^+$ T and $B220^+$ B cells from diseased CD40L/B Tg mice, whereas mice reconstituted with both $B220^+$ B cells and $CD4^+$ T cells from WT mice did not. This indicates that Tg B cells should be involved as a trigger for this colitis model. These observations demonstrate that the CD40-CD40L interaction among B cells may introduce abnormal Ig isotype switching and consecutive B cell expansion and may contribute to the infiltration in gut. Thus, this experimental murine model seems to be sharply distinct from any established murine IBD models in which dysregulative function of T cells and macrophages/dendritic cells should be an essential pathogenic mechanism.

Materials and Methods

Mice

CD40L/B Tg mice expressing CD40L on B cells were previously established by injecting the DNA fragment containing the CD40L cDNA, a V_H promoter, the IgH intron enhancer, and the Igκ3′ enhancer into C57BL/6 fertilized eggs (24). $CD40^{-/-}$ mice were described previously (25). In the present study male, 4- to 20-wk-old CD40L/B Tg mice and WT littermate controls were used. CD40L/B Tg×$CD40^{-/-}$ double-mutant mice were also generated. The animals were housed under specific pathogen-free conditions. All experiments were approved by the regional animal study committees. Cross-breeding of these mice was performed, and the presence of each transgene was identified by tail DNA.

Histopathology and immunohistochemical analysis

Tissue specimens were fixed in 10% neutral-buffered formalin and embedded in paraffin. Sections were stained with H&E. For the immunohistochemistry, sections were embedded in OCT compound (Tissue-Tek; Miles, Elkhart, IN), snap-frozen in liquid nitrogen, and stored at −80°C. Six-micron sections were incubated with primary Abs. These included anti-murine CD4 (RM4-5, rat IgG1; BD PharMingen, San Diego, CA), anti-murine CD8 (53-6.7, rat IgG2a; BD PharMingen), anti-murine B220 (RA3-6B2, rat IgG2a; BD PharMingen), anti-murine CD11c (HL-3, hamster IgG; BD PharMingen), and anti-F4/80 (A3-1, rat IgG2b; Serotec, Oxford, U.K.). Isotype-matched control Abs (BD PharMingen) were also used. Biotinylated goat anti-hamster IgG or rat anti-mouse IgG (BD PharMingen) was chosen as second Abs. After three washes with PBS, positively stained cells were detected by streptavidin-biotinylated HRP complex (Vectastain ABC kit; Vector Laboratories, Burlingame, CA), and visualized by diaminobenzidine. Then the sections were counterstained with hematoxylin.

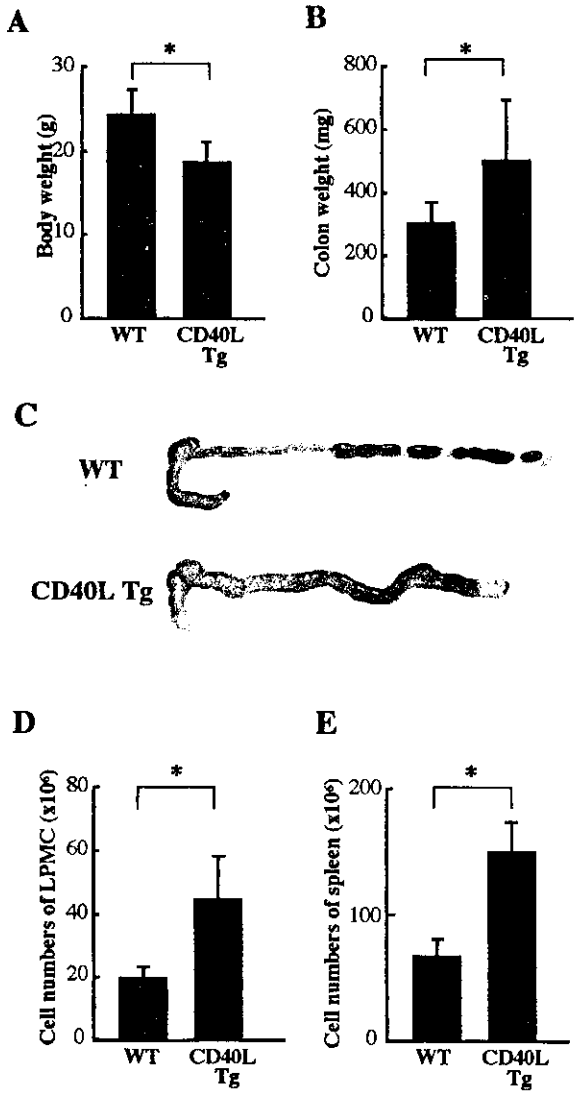

FIGURE 1. CD40L/B Tg mice developed the wasting disease with local and peripheral expansive cell growth. *A*, Approximately 90% of CD40L/B Tg mice (n = 29) had diarrhea and showed significant weight loss compared with WT littermates (n = 24) at 15 wk of age. *B*, The colonic weight of CD40L/B Tg mice was markedly larger than that of WT littermates at 15 wk of age. *C*, The macroscopic appearance of colon of CD40L/B Tg mice was enlarged, shortened, and had a greatly thickened wall compared with that of WT littermates. *D*, LPMCs were isolated from the colon of 15-wk-old CD40L/B Tg mice or their littermates, and the number of LPMCs was determined. Data are the mean ± SD of seven mice in each group. *E*, Splenocytes (Sp) were isolated from the colon of 15-wk-old CD40L/B Tg mice or their littermates, and the number of Sp was determined. *, $p < 0.05$.

Immunofluorescence analysis

In some experiments frozen sections of colon were prepared and fixed with cold acetone and then incubated with Block Ace (Dainippon-Pharmaceuticals, Tokyo, Japan). Sections were incubated with FITC-labeled goat anti-mouse IgM (magnification, ×500; Southern Biotechnology Associates, Birmingham, AL), tetramethylrhodamine (TRITC)-labeled goat anti-mouse IgG (magnification, ×500; Southern Biotechnology Associates), and biotin-labeled goat anti-mouse IgA (magnification, ×400; BD PharMingen), followed by incubation with aminocumarin-labeled streptavidin (magnification, ×500;

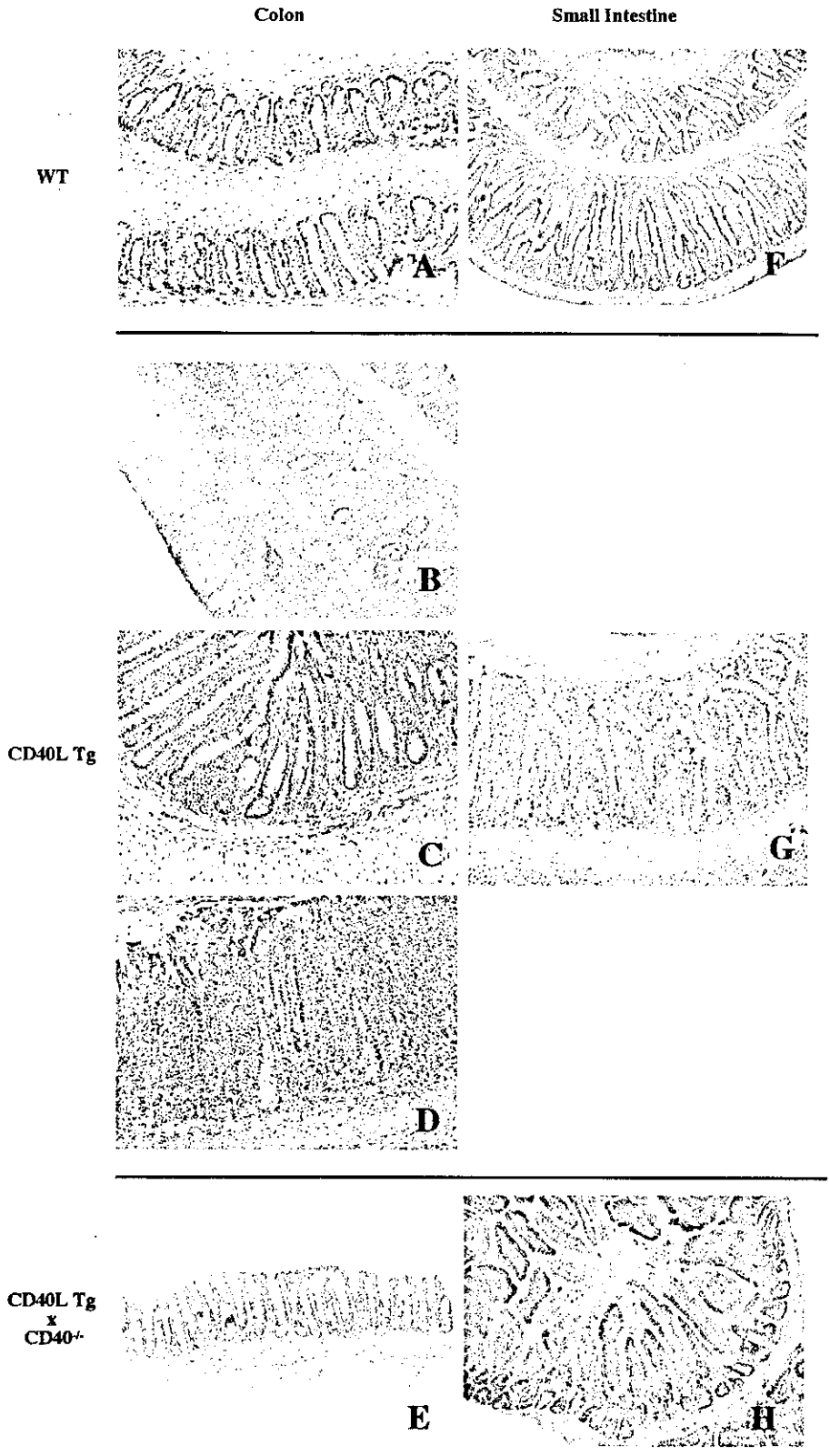

FIGURE 2. Histopathologic examination revealed the development of severe enterocolitis in CD40L/B Tg mice. Colons from WT littermates (*A*), CD40L/B Tg mice (*B–D*), and CD40L/B Tg×CD40$^{-/-}$ (*G*) mice and small intestines from WT littermates (*E*), CD40L/B Tg mice (*F*), and CD40L/B Tg×CD40$^{-/-}$ mice (*H*) were stained with H&E. Original magnification: *A*, *B*, *E–G*, and *H*, × 40; *C* and *D*, ×100.

Southern Biotechnology Associates) (26). Anti-colon autoantibodies in sera from 12- to 15-wk-old colitic CD40L/B Tg mice were detected by indirect immunofluorescence using colonic tissues from 6-wk-old nondiseased CD40L/B Tg mice. Sections were blocked with 10% goat serum in PBS for 30 min at room temperature and incubated with mouse serum diluted in 10% goat serum in PBS for 1 h, and then bound Ab was detected with TRITC-labeled anti-mouse IgG or FITC-labeled anti-mouse IgM. Sections were examined with a fluorescence microscope (BX50/BXFLA; Olympus, Tokyo, Japan) equipped with a charge-coupled device camera (Olympus) and an image capture system (Olympus). Combination images for multicolor staining were performed using Photoshop 4.0 (Adobe Systems, San Jose, CA).

Serum Ig

Total amounts of serum IgM, IgG, and IgA were measured by standard sandwich ELISA analysis using goat anti-IgM or IgG or IgA Abs (Southern Biotechnology Associates). Abs bound to the plates were detected using

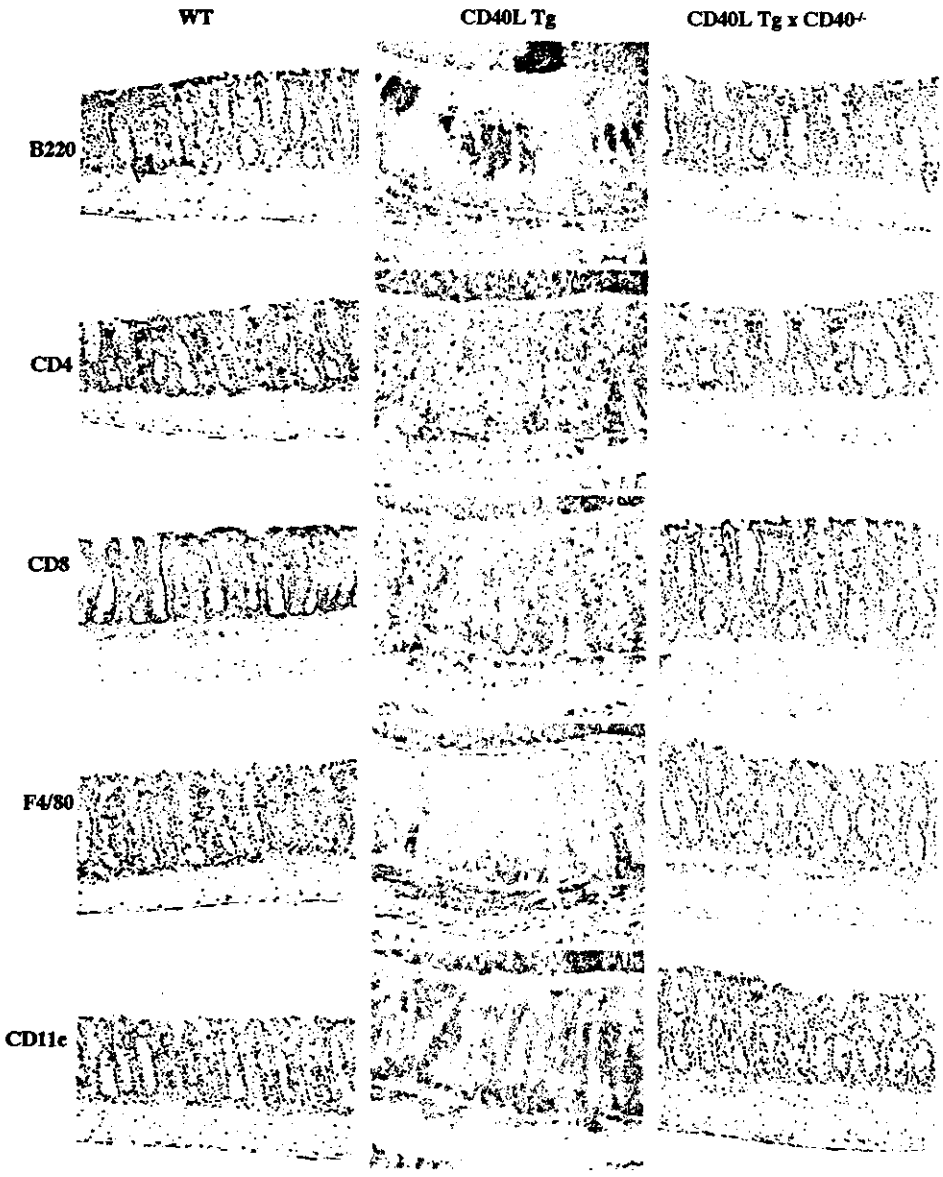

FIGURE 3. Immunohistochemical analysis showed the massive B220-positive cell infiltration to colonic tissue in CD40L/B Tg mice. A large number of aggregated $B220^+$ cells, which were structurally different from B cells in colonic patches, were infiltrated in the LP of diseased CD40L/B Tg mice. In addition, $CD4^+$, $CD8^+$, $F4/80^+$, and $CD11c^+$ cells were increased in the inflamed colonic mucosa of CD40L/B Tg mice compared with those of WT littermates or CD40L/B Tg×$CD40^{-/-}$ mice. Original magnification, ×100.

alkaline phosphatase-labeled anti-IgG, anti-IgM (BD PharMingen), and anti-IgA Abs (Southern Biotechnology Associates).

Cell preparation

LP mononuclear cells (LPMC) were isolated from the colon as described previously (27, 28). Briefly, the entire colon was opened longitudinally, washed with PBS, and cut into small pieces. The pieces were then incubated with Ca^{2+}- and Mg^{2+}-free HBSS containing 2.5% FBS and 1 mM DTT (Sigma-Aldrich, St. Louis, MO) for 30 min to remove mucus and then serially incubated twice in Ca^{2+}- and Mg^{2+}-free HBSS containing 2.5% FBS and 0.75 mM EDTA (Sigma-Aldrich) for 1 h each. The supernatants from these incubations were collected, pooled, and treated with 1 mg/ml collagenase (Worthington Biomedical, Freehold, NJ) and 0.01% DNase (Worthington Biomedical) in medium for 2 h. The cells were pelleted twice through a 40% isotonic Percoll solution and then further purified by Ficoll-Hypaque density gradient centrifugation (40/75%) at the interface.

Flow cytometry

The isolated LPMC were preincubated with an FcγR-blocking mAb (CD16/32; 2.4G2; BD PharMingen) for 20 min, followed by incubation with FITC-, PE-, or biotin-labeled mAb for 30 min on ice. Biotinylated Abs were detected with PE-streptavidin (BD Biosciences, Mountain View, CA). Two-color flow cytometric analysis was performed on a FACSCalibur (BD Biosciences) using CellQuest software. Background fluorescence was assessed by staining with isotype-matched control mAbs.

Cytokine analysis

Ninety-six-well culture plates were precoated with anti-CD3 mAb (5 μg/ml; 145-2C11; BD PharMingen) and anti-CD28 mAb (2 μg/ml; 37.51; BD PharMingen) in 100 μl of PBS at 37°C for 4 h and washed with PBS three times to remove unbound Abs. LP $CD4^+$ T cells (5×10^5/well) were then incubated at 37°C in 5% CO_2 humidified air for 48 h. Culture supernatants of littermate mice and Tg mice after onset of disease were harvested and assayed for IFN-γ and IL-4. Cytokine concentrations were determined by a specific ELISA kit for mouse IFN-γ and IL-4 (Endogen, Cambridge, MA). ODs were measured on an Intermet ELISA reader at a wavelength of 490 nm.

Adoptive transfer experiment

Adult female C57BL/6J SCID mice (6–8 wk old) were used as recipients in the following experiments. Diseased CD40L/B Tg and control WT littermates were euthanized at 18 wk of age. To obtain $CD4^+$ T or $B220^+$ B cells from the pooled splenocytes and mesenteric lymph node cells, $CD4^+$ T cells were purified using the anti-CD4 (L3T4) MACS beads (Miltenyi Biotec, Auburn, CA), and thereafter $B220^+$ cells were purified from the negatively selected $CD4^-$ cells using anti-B220 (RA3-6B2) MACS beads (Miltenyi Biotec). After the enriched $CD4^+$ T cells (96–97% pure, as estimated by FACSCalibur) and $B220^+$ B cells (95–96% pure) were labeled with PE-conjugated anti-mouse CD4 (RM4-5) and FITC-conjugated anti-B220 (RA3-6B2) mAbs, and the purified $CD4^+$ T cells and $B220^+$ B

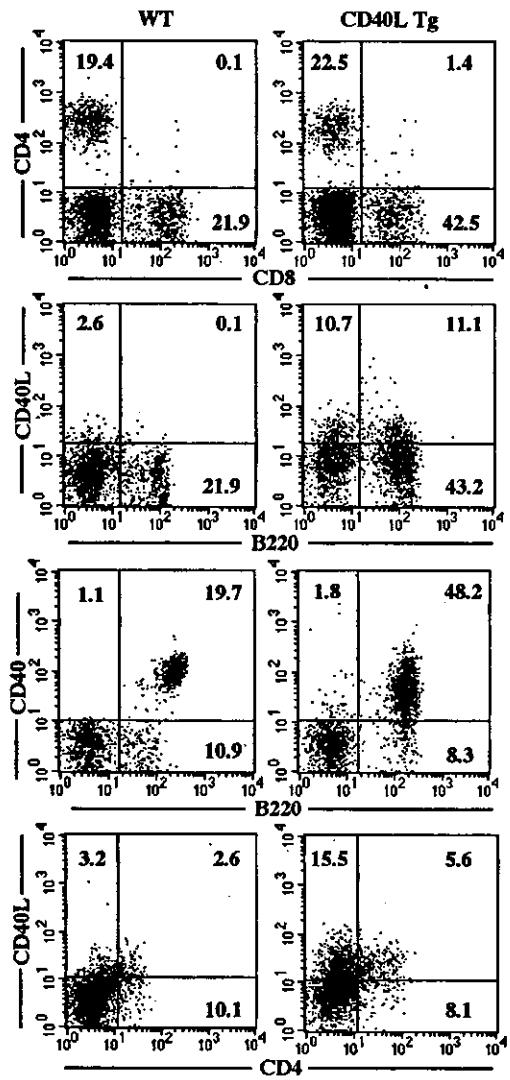

FIGURE 4. Flow cytometric analysis of LPMC from diseased CD40L/B Tg mice and WT littermates. The percentages of $CD8^+$ cells and the CD8/CD4 ratio were significantly increased in LPMC from diseased CD40L/B Tg mice compared with those from WT littermates. In CD40L Tg mice, the percentages of $B220^+$ LPMC were significantly increased and the expression of CD40L on B220-expressing LP B cells was also significantly up-regulated compared with those in WT littermates. In contrast, there were no differences in CD40 expression on LP B cells between CD40L/B Tg mice and littermates. Although we used the B cell-specific promoter and enhancer to establish CD40L/B Tg mice, CD40L/B on LP T cells in diseased mice was also slightly up-regulated compared with that in littermates. These data were representative of three experiments.

cells were then sorted by two-color sorting on a FACS Vantage (BD Biosciences). All populations were >99.0% pure on reanalysis. SCID mice were then injected i.p. with one or two subpopulations of the sorted $CD4^+$ T cell and/or $B220^+$ B cells in PBS: 1) CD40L/B Tg $B220^+$ (5×10^5/mouse), 2) CD40L/B Tg $CD4^+$ (5×10^5/mouse), 3) CD40L/B Tg $B220^+$ (5×10^5/mouse) and CD40L/B Tg $CD4^+$ (5×10^5/mouse), 4) CD40L/B Tg $B220^+$ (5×10^5/mouse) and WT $CD4^+$ (5×10^5/mouse), 5) WT $B220^+$ (5×10^5/mouse) and WT $CD4^+$ (5×10^5/mouse), 6) WT $B220^+$ (5×10^5/mouse), 7) WT $CD4^+$ (5×10^5/mouse), or 8) no transfer control. Mice were killed and analyzed 4 wk after transfer, and the colons were removed and evaluated histologically. For the histological score, the area of the proximal colon was scored on a scale of 0–3 in each of three criteria: cell infiltration, crypt elongation, and crypt abscesses. Histological grades were assigned in a blind fashion by one pathologist (R.I.).

Statistical analysis

Data were expressed as the mean and SD and are plotted in corresponding figures. The differences between experimental groups were statistically analyzed with the Mann-Whitney U test. A value of $p < 0.05$ was considered significant.

Results

CD40L/B Tg mice developed a wasting disease with severe intestinal inflammation

Clinical manifestation was monitored for up to 30 wk. IBD symptoms were first observed between 8 and 15 wk of age. Approximately 90% of CD40L/B Tg mice had diarrhea and developed significant weight loss until 20 wk of age ($p < 0.05$; Fig. 1*A*). In contrast, their WT littermates appeared healthy, with a gradual increase in body weight and absence of diarrhea during the period of observation (Fig. 1*A*). Macroscopic appearance showed enlarged colon with a greatly thickened wall in CD40L/B Tg mice (Fig. 1*C*), and the colonic weight of 15-wk-old CD40L/B Tg mice was significantly increased compared with that of littermates ($p < 0.005$; Fig. 1*B*). In addition, the spleen and mesenteric lymph node enlargement was also present in diseased CD40L/B Tg mice (data not shown). Consistent with these data, the numbers of mononuclear cells recovered from the colon and spleen of 15-wk-old CD40L Tg mice were significantly increased compared with those of their littermates (Fig. 1, *D* and *E*), indicating extensive mononuclear cell proliferation in the inflamed colon and spleen of CD40L/B Tg mice.

Histopathologic examination of colonic tissue revealed the development of severe colitis in 15-wk-old CD40L/B Tg mice (Fig. 2, *B–D*). Large numbers of mononuclear cells infiltrated transmurally in colonic mucosa (Fig. 2*B*). Prominent epithelial hyperplasia with glandular elongation (Fig. 2*C*) and goblet cell depletion (data not shown) were common in whole colon. Extensive leukocytic infiltrates were seen in the LP and submucosa and, to a lesser degree, in the muscularis, serosa, and mesentery (Fig. 2, *B* and *D*). The mucosal abnormalities, such as thickening of the intestinal wall, virous atrophy, crypt hyperplasia, and infiltrations of mononuclear cells were also seen in the ileum of CD40L/B Tg mice (Fig. 2*G*). Splenomegaly with large amounts of lymphocytes and markedly enlarged mesenteric lymph nodes were present in these colitic mice (data not shown). In contrast, colonic and ileac sections from WT littermates showed few lymphocytes and macrophage infiltration in LP (Fig. 2, *A* and *F*). To determine whether these abnormalities in CD40L/B Tg mice was really due to the direct CD40-CD40L interaction in vivo, we next generated CD40L/B Tg×$CD40^{-/-}$ double-mutant mice. These mice were monitored for up to 30 wk, but they appeared healthy with a gradual increase in body weight and the absence of diarrhea during the period of observation (data not shown). In addition, colonic and ileac sections from age-matched CD40L/B Tg×$CD40^{-/-}$ mice showed few lymphocytes and macrophage infiltration in the LP (Fig. 2, *E* and *H*).

To examine the phenotypical cell surface markers of infiltrated mononuclear cells, the sections of colon were immunohistochemically stained with Abs against B220, CD4, CD8, F4/80, and CD11c. The major population of cell infiltrates was $B220^+$ cell aggregates, which were structurally different from colonic patches. B cells were markedly infiltrated in the LP from diseased CD40L/B Tg mice as well as serosa and mesentery (Fig. 3). In addition, $CD4^+$, $CD8^+$, $F4/80^+$, and $CD11c^+$ cells in the inflamed mucosa from diseased CD40L/B Tg mice were increased in the inflamed colonic mucosa compared with those from WT littermates (Fig. 3). Unlike most reported animal models of IBD, $CD8^+$ T cells seemed to infiltrate to a greater extent in inflamed mucosa

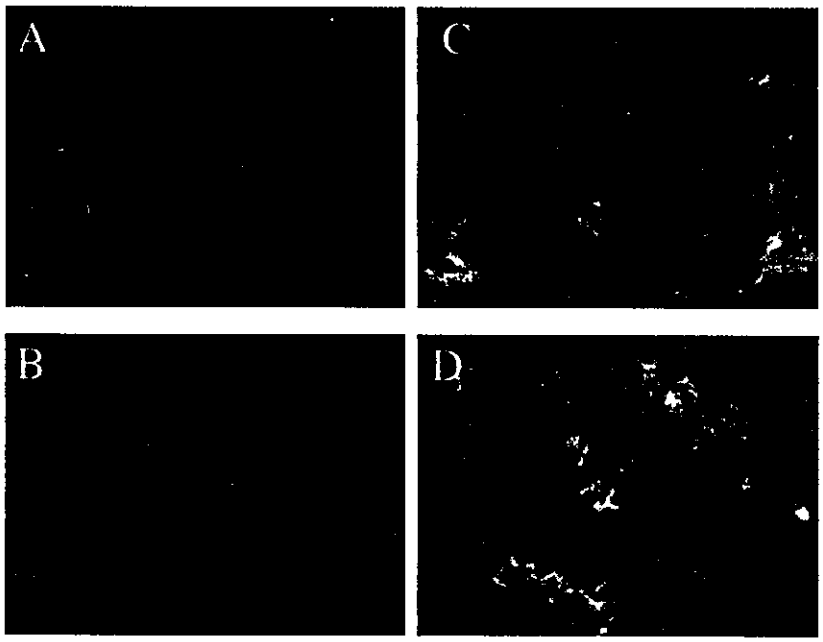

FIGURE 5. Colonic Ig-producing cells in CD40L/B Tg mice. Fifteen-week-old WT littermates (*A*), 6-wk-old nondiseased CD40L Tg mice (*B*), and 15-wk-old diseased CD40L/B Tg mice (*C* and *D*) were stained for IgG (red), IgM (green), and IgA (blue) by fluorescent immunohistochemistry. Diseased and nondiseased CD40L/B mice had almost similar numbers of IgA plasma cells in colon as WT littermates. In contrast, a markedly increased number of IgM^+ cells was observed in inflamed mucosa in diseased CD40L/B Tg mice. In addition, the number of IgG-producing cells in diseased CD40L/B Tg mice was slightly, but significantly, increased compared with those in nondiseased CD40L/B Tg mice and WT littermates. Original magnification: *A–C*, ×200; and *D*, ×1000. These data were representative of three experiments.

compared with $CD4^+$ T cells. In contrast, the littermates and age-matched CD40L/B Tg×$CD40^{-/-}$ mice showed no obvious infiltration of $B220^+$, $CD4^+$, $CD8^+$, $F4/80^+$, or $CD11c^+$ cells in the colon (Fig. 3).

Autoimmune diseases are often associated with the involvement of other organs, in particular the kidneys and sometimes the lungs, during disease progression. Therefore, cryostat sections of various tissues were analyzed for the presence of inflammation. Approximately half the CD40L/B Tg mice showed apparent glomerulonephritis and hyperplastic bronchus-associated lymphoid tissue in lungs (data not shown). However, no inflammation in other organs, such as skin, submaxillary gland, heart, liver, pancreas, and stomach, were observed (data not shown).

Increased expression of CD40L on B cells in diseased CD40L/B Tg mice

Flow cytometric analysis of LPMC from colitic mice showed that the percentages of $B220^+$ LPMC were significantly increased compared with those in WT littermates (Fig. 4). Consistent with immunohistochemical studies, unlike other T cell-mediated colitis models, the percentages of $CD8^+$ cells and the CD8:CD4 ratio were significantly increased compared with those in WT littermates (Fig. 4). In diseased CD40L/B Tg mice, the expression of CD40L on B220-expressing LP B cells was significantly up-regulated. The mean fluorescein intensity of $B220^+CD40L^+$ LP B cells in CD40L/B Tg mice was much higher than that in young nondiseased CD40L/B Tg mice (data not shown). In contrast, there were no differences in CD40 expression on B cells between CD40L/B Tg mice and littermates (Fig. 4). Although we used the B cell-specific promoter and enhancer to establish CD40L/B Tg mice, CD40L on LP T cells in diseased, but not in nondiseased, CD40L/B Tg mice was also up-regulated compared with that in littermates (Fig. 4). These data indicated that CD40L expression on T cells could be secondary to the response to inflammatory actions in colon.

To further investigate the role of CD40L-expressing B cells in the development of colitis in CD40L/B Tg mice, we assessed Ig-producing cells using confocal fluorescent immunohistochemistry. As shown in Fig. 5, diseased and nondiseased CD40L/B Tg mice had almost similar numbers of IgA plasma cells in colon compared with WT littermates. In contrast, it was of note that there was markedly increased number of surface IgM-positive cells were observed in inflamed mucosa in diseased CD40L/B Tg mice (Fig. 5). In addition, surface IgG-producing cells, which were rarely present in LP, were often detected in diseased CD40L/B Tg compared with nondiseased CD40L/B Tg mice (Fig. 5).

To next assess the systemic Ig production in CD40L/B Tg mice, we tested concentrations of serum IgG, IgM, and IgA using the specific sandwich ELISA. As shown in Fig. 6, concentrations of serum IgG and IgM were significantly increased by 4- and 5-fold, respectively, in diseased CD40L/B Tg mice compared with WT littermates (IgG; $p < 0.005$, IgM; $p < 0.05$). In some diseased CD40L/B Tg mice, serum IgA was increased, but not significantly different ($p = 0.29$).

Anti-colon autoantibodies

To assess the involvement of anti-colon autoantibodies in the pathogenesis of colitis, we tested whether sera obtained from colitic mice react with epithelial cells in the uninflamed colon of young nondiseased CD40L/B Tg mice. As shown in Fig. 7, both anti-colon IgG and IgM autoantibodies were detected in sera from colitic mice, IgM autoantibody reacted with crypt epithelium, and IgG autoantibody showed strong reaction with surface epithelium of the colon. These reactivities were seen with 1/125 diluted sera from diseased CD40L/B Tg mice. In contrast, staining of epithelial cells was not seen with sera from nondiseased mice and WT littermates at 1/25 or 1/125 dilution (Fig. 7).

B1/B2 differentiation in CD40L/B Tg mice

Based on the involvement of autoantibodies against intestinal epithelial cells in sera derived from diseased CD40L/B Tg mice, we further assessed B1 B cells in inflamed mucosa, because B1 cells appears to produce Abs in a T cell-independent manner (29). Flow cytometric analysis of LPMC from colitic mice showed no significant absolute increase in $CD5^+IgM^+$ B1 B cells on LPMC from diseased CD40L/B Tg mice (percentage of $CD5^+IgM^+$/lymphocyte gate: WT, 0.4 ± 0.2%; CD40L/B Tg, 0.9 ± 0.5%; $p = 0.18$), indicating that autoantibody production could require T cell-dependent help or the involvement of nonmucosal B1 B cells, which may be located in peritoneal and pleural cavities.

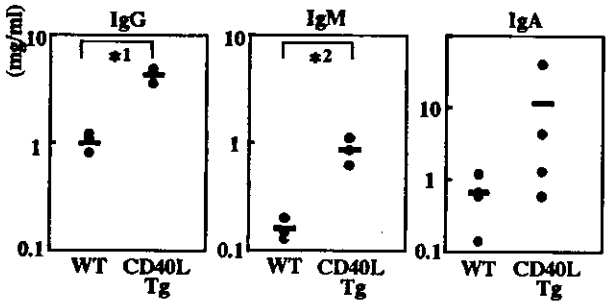

FIGURE 6. Serum concentrations of Igs from CD40L/B Tg mice (n = 4) and WT littermates (n = 4) at 18 wk of age. Serum IgG, IgM, and IgA were measured using the specific sandwich ELISA. The average concentrations of serum IgG and IgM were significantly increased by 4- and 5-fold, respectively, in diseased CD40L/B Tg mice compared with WT littermates. In some diseased CD40L/B Tg mice, serum IgA was markedly increased, but the difference was not significant (p = 0.29). *1, $p < 0.05$, *2, $p < 0.005$.

Th1-mediated immune responses in CD40L/B mice

As mentioned above (Fig. 4), $CD4^+$ and $CD8^+$ T cells were also increased in inflamed mucosa from diseased CD40L/B Tg mice. We then assessed the involvement of Th cells in the development of this colitis. Isolated LP $CD4^+$ T cells were cultured, and the supernatants were analyzed for concentrations of IFN-γ and IL-4 by specific ELISA. IFN-γ ($p < 0.05$), but not IL-4, production by anti-CD3/anti-CD28 mAbs-stimulated LP $CD4^+$ T cells was significantly increased in diseased CD40L/B Tg compared with WT littermates (IFN-γ: WT, 12.1 ± 3.0 ng/ml; CD40L/B Tg, 84.8 ± 12.1 ng/ml (p = 0.001); IL-4: WT, 575.2 ± 75.0 pg/ml; CD40L/B Tg, 469.0 ± 75.9 pg/ml (p = 0.68)), indicating that colitis induced in CD40L/B Tg mice could be mediated in secondary Th1-immune responses.

Adoptive transfer experiments

To establish which cell type mediates the inflammation in CD40L/B Tg mice, we next performed the adoptive transfer experiments using sorted B and T cells from diseased CD40L/B Tg and WT littermate mice in the indicated protocol (Fig. 8*A*). As shown in Fig. 8*B*, mice transferred with CD40L/B Tg $CD4^+$ T cells alone or with both CD40L/B Tg $CD4^+$ T and CD40L/B Tg $B220^+$ B cells, but not CD40L/B Tg $B220^+$ cells alone, develop colitis 4 wk after transfer, indicating that the final cause of colitis is the dysregulated $CD4^+$ T cells. However, mice reconstituted with CD40L/B Tg $B220^+$ B cells and WT $CD4^+$ T cells also developed colitis, whereas mice reconstituted with both WT $B220^+$ B cells and WT $CD4^+$ T cells did not. These differences were confirmed by histological scoring of multiple colon sections obtained from five mice in each group (Fig. 8*C*). This indicates that Tg B cells should be a trigger for this colitis model, and thereafter, dysregulated $CD4^+$ T cells are also needed as final effectors.

Discussion

This report describes a novel model of intestinal pathology induced by primarily B cell-triggered mechanism. To date, studies in animal models of IBD have mainly focused on $CD4^+$ T cells of unknown specificity and in part dendritic cells/macrophages (30) and $CD8^+$ T cells (31). In this study we show that abnormal B cells expressing CD40L can also trigger chronic colitis and may provide a link with autoimmune intestinal inflammation.

It is generally established that the interaction of CD40L on activated T cells with CD40 on APC leads to the secretion of IL-12 by APC, including dendritic cells and macrophages (32–37), and that such interactions are critical for IL-12 production in Ag-driven responses of animal models of colitis (12, 38, 39) and human IBD (9). In contrast, there were no reports that mentioned the involvement of CD40L-expressing B cells in IBD despite some evidence that CD40L is expressed on B cells as well as T cells in patients with SLE (21), and ectopic expression of CD40L on B cells has been observed in lupus-prone BXSB mice (40). The expression of CD40L is activation dependent; CD40L appears on the cell surface within 1–3 h after Ag recognition, and then immediately disappears by 24 h (7). In fact, it was difficult to detect CD40L on any type of cell, probably because CD40L expression in nondiseased young CD40L/B Tg mice was down-regulated in the presence of CD40 as described previously (25, 41). Indeed, we could detect surface expression of CD40L using CD40L/B Tg mice crossed with CD40-deficient mice in the spleen, lymph nodes, and bone marrow (Y. Aiba, details will be described elsewhere). Further study will be required to determine whether CD40L could be expressed on B cells in inflamed mucosa from patients with IBD as well as activated T cells, although it could be technically hard to determine this. Of importance, isolated LPMC from IBD mucosa have been reported to contain more B cells, particularly B cells producing IgG, compared with noninvolved IBD mucosa or control mucosa (42). Furthermore, circulating autoantibodies produced by abnormal B cells, such as colon epithelial cells and leukocyte nuclei, have been consistently identified in patients with UC or CD (43). The accumulating evidence led us to investigate the possible role of CD40L on B cells in the primary development of colitis using CD40L/B Tg mice expressing CD40L ectopically on B cells.

In the present study we demonstrate that CD40L/B Tg mice expressing CD40L on B cells develop chronic enterocolitis, which is first observed between 8 and 15 wk of age with massive infiltration of aggregated IgM-producing B cells in LP, and produce autoantibodies against colonic epithelial cells. First, we postulated that abnormal CD40-CD40L B-B interaction might be induced by ectopic expression of CD40L on B cells and may introduce 1) abnormal Ig isotype switching, 2) consecutive IgM-positive B cell proliferation, and 3) infiltration in the gastrointestinal tract. In contrast, T cells also infiltrate inflamed lesions, but the degree is much less than that of B cells. Interestingly, unlike most other animal models of colitis (1, 5), the CD4/CD8 ratio of LP T cells of inflamed colon was significantly decreased compared with that in WT littermates. These results indicated that CD40L/B Tg mice are sharply distinct from any established T cell/macrophages/dendritic cell-mediated murine models of intestinal inflammation.

Similarly, Clegg et al. (11) reported that CD40L Tg mice overexpressing CD40L on T cells (CD40L/T Tg) acquire a lethal chronic colitis marked by the infiltration of $CD40L^+$ T cells and $CD40^+$ cells into diseased tissues. Interestingly, they showed abnormal thymus development in CD40L/T Tg, such as a transgene copy-dependent decline in thymocyte number, loss of cortical epithelium, and expansion of $CD40^+$ medullary cells (11). In their model they postulated that CD40L/T Tg failed to develop regulatory T cells in thymus that suppress the development of colitis by abnormal T cell development. In addition to a defect in thymic negative selection in CD40L/T Tg, the chronic inflammation in colon might be caused by the continuation of transgene expression in peripheral T cells (11). In contrast, our CD40L/B Tg expressing CD40L on B cells showed no abnormalities in thymus in either flow cytometric or histological analysis (data not shown), indicating that not only could chronic intestinal inflammation in our CD40L/B Tg mice expressing CD40L on B cells be mediated in a thymus-independent manner, but also the CD40L transgene system

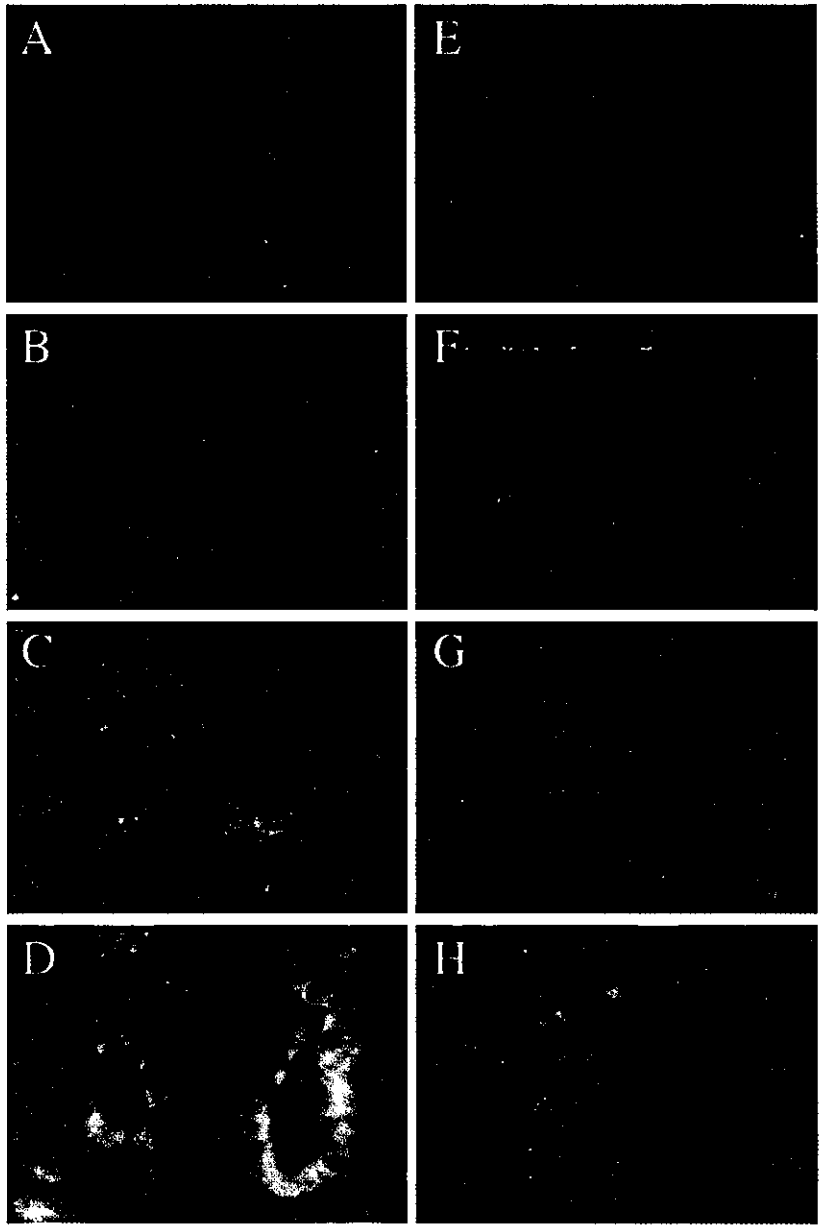

FIGURE 7. Anti-colon Abs were detected in sera from diseased CD40L/B Tg mice. Sera obtained from 12- to 15-wk-old colitic mice stained some surface epithelial cells in the uninflamed colon of young nondiseased CD40L/B Tg mice (*C* and *F*), but this was not observed when sera from WT littermate mice (*A* and D) and nondiseased young CD40L/B Tg mice (*B* and *E*) were used. For the detection of IgM (*A–D*) and IgG type (*E–H*) autoantibodies, FITC-labeled anti-mouse IgM and TRITC-labeled anti-mouse IgG, respectively, were used for the second antibodies. Original magnification: *A–C* and *E–G*, ×200; and *D* and *H*, ×1000. These data were representative of three experiments.

does not introduce CD40L expression into T cells because of the use of a B cell-specific promoter. Nevertheless, the fact that we detected CD40L protein on LP $CD4^+$ T cells from diseased CD40L/B Tg mice suggested that the expression of CD40L on LP $CD4^+$ T cells might be secondary in the reaction against the local intestinal inflammation. Indeed, like most CD40L-mediated animal models of IBD (9, 10, 12–14), LP $CD4^+$ T cells in inflamed mucosa from diseased CD40L/B Tg mice showed IFN-γ-dominant, rather than IL-4-dominant, cytokine production, indicating that our mice might be a good Th1-mediated chronic colitis model. It is also possible that CD40L-expressing LP B cells could directly stimulate CD40-expressing dendritic cells/macrophages to produce IL-12 and to introduce Th1-mediated immune responses. To determine the role of CD40L on B cells in the development of colitis in this model, we next performed an adoptive transfer of isolated T or B cells from diseased CD40L/B Tg and WT littermate mice into SCID mice. We demonstrated that mice transferred with $CD4^+$ T cells alone or with both $CD4^+$ T and $B220^+$ B cells, but not $B220^+$ cells alone, from diseased CD40L/B Tg mice develop colitis, indicating that the final cause of colitis is the dysregulated $CD4^+$ T cells. However, we also demonstrated that mice transferred with $B220^+$ B cells from diseased CD40L/B Tg mice and $CD4^+$ T cells from WT mice also developed colitis, whereas mice transferred with both $B220^+$ B cells and $CD4^+$ T cells from WT mice did not. This indicates that the Tg B cells should be involved in this colitis as a trigger for this colitis model. It should be noted that this transfer experiment also clearly excluded the possibility that the Tg CD40L was expressed on T cells in our Tg system.

In our CD40L/B Tg mice, serum IgM and IgG concentrations were 4- to 5-fold increased. Intestinal mucosal plasma cells producing IgG or IgM were apparently increased, but the number of IgA-producing cells was not significantly different compared with that in WT littermates. Comparison with the findings in human tissue from patients with IBD and in some experimental colitis models reveals some similarities. In human IBD, levels of IgG and IgM are increased along with disease progression. In contrast, it has been demonstrated the level of IgA is decreased in patients with chronic UC (44) and CD (45), but increased in the quiescent disease (46). Furthermore, we detected IgM- and IgG-type autoantibodies

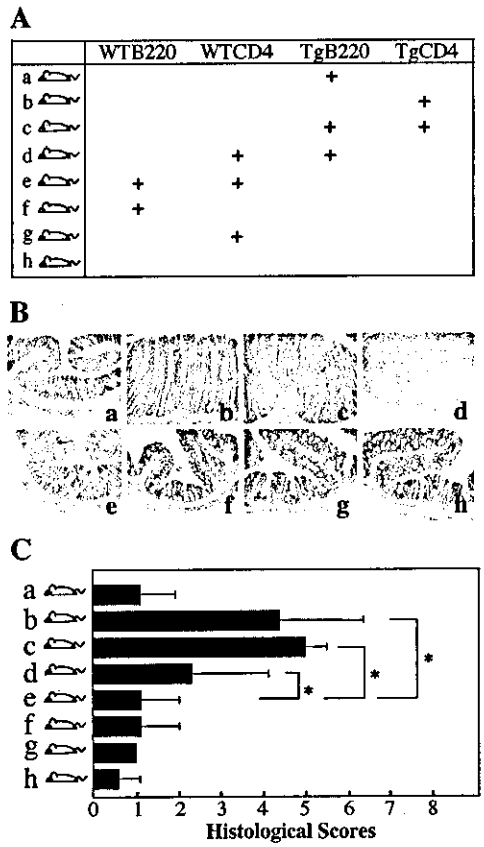

FIGURE 8. Adoptive transfer of sorted T and B cells obtained from spleens and mesenteric lymph nodes. *A*, Transfer protocol. C57BL/6 SCID mice were injected i.p. with one or two of the indicated subpopulations of sorted $CD4^+$ T cells and $B220^+$ B cells from diseased CD40L/B Tg mice (18 wk old) and WT littermates: a, CD40L/B Tg $B220^+$ (5×10^5/body); b, CD40L/B Tg $CD4^+$ (5×10^5/body); c, CD40L/B Tg $B220^+$ (5×10^5/body) and CD40L/B Tg $CD4^+$ (5×10^5/body); d, CD40L/B Tg $B220^+$ (5×10^5/body) and WT $CD4^+$ (5×10^5/body); e, WT $B220^+$ (5×10^5/body) and WT $CD4^+$ (5×10^5/body); f, WT $B220^+$ (5×10^5/body); g, WT $CD4^+$ (5×10^5/body); or h, no transfer control. Mice were euthanized 4 wk after transfer. *B*, Histopathology of distal colon from each mice. Original magnification, ×100. *C*, Histological scores were determined 4 wk after transfer as described in *Materials and Methods*. Data are presented as the mean ± SD (n = 5). *, $p < 0.05$.

against colonic epithelial cells. T cell-dependent immune responses generally involve conventional B2 B cells. In contrast, the other subset of B cells, B1 B cells, appear to produce Abs in a T-independent manner (27, 47, 48). B1 B cells, originally defined by the surface expression of CD5 and high levels of IgM, arise early in ontogeny, home predominantly to the peritoneal and pleural cavities, have a capacity for self-renewal, and display different receptor specificities. B1 cells appear to recognize self-Ag as well as common bacterial Ags. Production of autoantibodies by B1 cells is also supported by the fact that the neoplastic expansion of B1 cells, such as in chronic lymphocytic leukemia, is often associated with autoimmune symptoms (26, 47, 48). Based on the evidence, we assessed whether autoantibodies are produced via T cell-dependent (B1; $CD5^+IgM^+$) or T cell-independent (B2; $CD5^-IgM^+$) fashion. We showed no increase in $CD5^+IgM^+$ B cells in inflamed mucosa from these mice compared with those in WT littermates, indicating that autoantibodies in diseased CD40L/B Tg mice might be produced by T cell-dependent B2 cells. Alternatively, the autoantibodies in this model could be generated in other tissues, such as peritoneal cavity. In addition, it should be noted that Mizoguchi and colleagues (49, 50) recently demonstrated that highly CD1d-expressing B cells were significantly increased in mesenteric lymph nodes from colitic $TCR\alpha^{-/-}$ mice and had a unique ability to produce IL-10. They postulated that these B cells functioned as regulatory B cells to suppress the progression of intestinal inflammation by down-regulating inflammatory cascades associated with IL-1 up-regulation and STAT3 activation (49, 50). Although there might be a correlation between their regulatory B cells and our pathogenic B cells in the development of colitis at this point, it seems likely that our aggregated IgM-producing, activated B cells in inflamed mucosa from diseased CD40L/B Tg mice did not possess such a regulatory function, but differentiated to more pathogenic cells in the early stage of colitis development. Further study will be required to assess the features of CD40L-expressing B cells, such as cytokine production and APC function.

In conclusion, the present data suggested that under some conditions the CD40-CD40L interaction is constitutively generated on B cells by themselves, and IBD pathogenesis might be established by a primarily B cell-triggered mechanism without involving mainly T cells or macrophages/dendritic cells. Further investigation, such as establishing double-mutant mice crossed between CD40L/B Tg mice and nude mice, may be beneficial to elucidate the primary involvement of B cells in the pathogenesis of IBD.

Acknowledgments

We express special thanks to Dr. Morio Koike for critical comments, and to Saeko Matsumoto for manuscript preparation.

References

1. Podolsky, D. K. 1995. Inflammatory bowel disease (first of two). *N. Engl. J. Med. 325:928.*
2. Fiocchi, C. 1998. Inflammatory bowel disease: etiology and pathogenesis. *Gastroenterology 115:182.*
3. Sartor, R. B. 1997. Pathogenesis and immune mechanism of chronic inflammatory bowel disease. *Am. J. Gastroenterol. 92:5S.*
4. Blumberg, R. S., L. J. Saubermann, and W. Strober. 1999. Animal models of mucosal inflammation and their relation to human inflammatory bowel disease. *Curr. Opin. Immunol. 11:648.*
5. Powrie, F. 1995. T cells in inflammatory bowel disease: protective and pathogenic role. *Immunity 3:171.*
6. Grewal, I. S., and R. A. Flavell. 1998. CD40 and CD154 in cell mediated immunity. *Annu. Rev. Immunol. 16:111.*
7. Banchereau, J., F. Bazan, D. Blanchard, F. Briere, J. P. Galizzi, C. van Kooten, Y. J. Liu, F. Rousset, and S. Saeland. 1994. The CD40 antigen and its ligand. *Annu. Rev. Immunol. 12:881.*
8. van Kooten, C., and J. Banchereau. 2000. CD40-CD40ligand. *J. Leukocyte Biol. 67:2.*
9. Zhanju, L., S. Colpaert, G. R. D'Haens, A. Kasran, M. D. Boer, P. Rutgeerts, K. Geboes, and J. L. Ceuppens. 1999. Hyperexpression of CD40 ligand (CD154) in inflammatory bowel disease and its contribution to pathogenic cytokine production. *J. Immunol. 163:4049.*
10. Battaglia, E., L. Bianocon, A. Resegotti, G. Emanuelli, G. R. Fronda, and G. Cammusi. 1999. Expression of CD40 and its ligand CD40L, in intestinal lesions of Crohn's disease. *Am. J. Gastroenterol. 94:3279.*
11. Clegg, C., J. T. Ruffles, H. S. Haugen, I. H. Hoggatt, A. Aruffo, S. Durham, and A. G. Farr. 1997. Thymus dysfunction and chronic inflammatory disease in gp39 transgenic mice. *Int. Immunol. 9:1111.*
12. Stuber, E., W. Strober, and M. Neurath. 1996. Blocking the CD40L-CD40 in vivo specifically prevents the priming of T helper 1 cells through the inhibition of interleukin 12 secretion. *J. Exp. Med. 183:693.*
13. Zhanju, L., K. Geboes, S. Colpaert, L. Overbergh, C. Mathieu, H. Heremans, M. D. Boer, L. Boon, G. D'Haens, P. Rutgeerts, et al. 2000. Prevention of experimental colitis in SCID mice reconstituted with $CD45RB^{high}CD4^+$ T cells by blocking the CD40-CD154 interactions. *J. Immunol. 164:6005.*
14. de Jong, Y., M. Comiskey, S. Kalled, E. Mizoguchi, R. A. Flavell, A. K. Bhan, and C. Terhorst. 2000. Chronic murine colitis is dependent on CD154/CD40 pathway and can be attenuated by anti-CD154 administration. *Gastroenterology 119:715.*
15. van Kooten, C., and J. Banchereau. 1997. Functions of CD40 on B cells, dendritic cells and other cells. *Curr. Opin. Immunol. 9:330.*
16. Foy, T. M., A. Aruffo, J. Bajorath, J. E. Buhlmann, and R. J. Noelle. 1996. Immune regulation by CD40 and its ligand gp39. *Annu. Rev. Immunol. 14:591.*
17. Koshy, M., D. Berger, and M. K. Crow. 1996. Increased expression of CD40 ligand on systemic lupus erythematosus lymphocytes. *J. Clin. Invest. 98:826.*

18. Takahashi, F., and K. M. Das. 1985. Isolation and characterization of a colonic autoantigen specifically recognized by colon tissue-bound immunogloblin G from idiopathic ulcerative colitis. *J. Clin. Invest. 76:311.*
19. Hibi, T., S. Aiso, M. Ishikawa, M. Watanabe, T. Yoshida, K. Kobayashi, H. Asakura, S. Tsuru, and M. Tsuchiya. 1983. Circulating antibodies to the surface antigens on colon epithelial cells in ulcerative colitis. *Clin. Exp. Immunol. 54:163.*
20. Sadlack, B., H. Merz, H. Schorle, A. Schimpl, A. C. Feller, and I. Horak. 1993. Ulcerative colitis-like disease in mice with a disrupted interleukin-2 gene. *Cell 75:253.*
21. Desai-Mehta, A., L. Lu, R. Ramsy-Goldman, and S. K. Datta. 1996. Hyperexpression of CD40 ligand by B and T cells in human lupus and its role in pathogenic autoantibody production. *J. Clin. Invest. 97:2063.*
22. Ishikawa, O., Y. Miyachi, K. Fujita, S. Takenoshita, Y. Nagamachi, and J. Hirato. 1995. Ulcereative colitis associated with preceding systemic lupus erthematosus. *J. Dermatol. 22:289.*
23. Koutroubakis, I. E., H. Kritikos, I. A. Mouzas, S. M. Spanoudakis, A. N. Kapsoritakis, E. Petinaki, E. A. Kouroumalis, and O. N. Manousos. 1998. Association between ulcerative colitis and systemic lupus erythematosus: report of two cases. *Eur. J. Gastroenterol. Hepatol. 10:437.*
24. Higuchi, T., Y. Aiba, T. Nomura, J. Matsuda, K. Mochida, M. Suzuki, H. Kikutani, T. Honjo, K. Nishioka, and T. Tsubata. 2002. Ectopic expression of CD40 ligand on B cells induces lupus-like autoimmune disease. *J. Immunol. 168:9.*
25. Kawada, T., T. Naka, K. Yoshida, T. Tanaka, H. Fujiwara, S. Suematsu, N. Yoshida, T. Kishimoto, and H. Kikutani. 1994. The immune responses in CD40-deficient mice: impaired immunoglobulin class switching and germinal center formation. *Immunity 1:167.*
26. Dohi, T., P. D. Rennert, K. Fujihashi, H. Kiyono, Y. Shirai, Y. I. Kawamura, J. L. Browning, and J. R. McGhee. 2001. Elimination of colonic patches with lymphotoxin β receptor-Ig prevents cell-type colitis. *J. Immunol. 167:2781.*
27. Totsuka, T., T. Kanai, R. Iiyama, K. Uraushihara, M. Yamazaki, R. Okamoto, T. Hibi, K. Tezuka, M. Azuma, H. Akiba, et al. 2003. Ameliorating effect of anti-inducible costimulator monoclonal antibody in a murine model of chronic colitis. *Gastroenterology 124:410.*
28. Bull, D. M., and M. A. Bookman. 1977. Isolation and functional characterization of intestinal mucosal lymphoid cells. *J. Clin. Invest. 59:966.*
29. Fagarasan, S., and T. Honjo. 2000. T-independent immune response: new aspects of B cell biology. *Science 6:89.*
30. Takeda, K., T. Kaisho, N. Terada, and S. Akira. 1999. Enhanced Th1 activity and development of chronic enterocolitis in mice devoid of Stat3 in macrophages and neutrophils. *Immunity 10:34.*
31. Steinhoff, U., V. Brinkmann, U. Klemm, P. Aichele, P. Seiler, U. Brandt, P. W. Bland, I. Prinz, U. Zugel, and S. H. E. Kaufmann. 1999. Autoimmune intestinal pathology induced by hsp60-specific CD8 T cells. *Immunity 11:349.*
32. Kamanaka, M., P. Yu, T. Yasui, K. Yoshida, T. Kawabe, T. Horii, T. Kishimoto, and H. Kikutani. 1996. Protective role of CD40 in *Leishmania major* infection at two distinct phases of cell mediated immunity. *Immunity 4:275.*
33. Campbell, K. A., P. J. Ovendale, M. K. Kennedy, W. C. Fanslow, S. G. Reed, and C. R. Maliszewski. 1996. CD40 ligand is required protective cell-mediated immunity to *Leishmania major. Immunity 4:283.*
34. Shu, U., M. Kiniwa, C. Y. Wu, C. Maliszewski, N. Vezzio, J. Hakimi, M. Gately, and G. Delespesse. 1995. Activated T cells induce interleukin-12 production by monocytes via CD40-CD40 ligand interaction. *Eur. J. Immunol. 25:1125.*
35. Simpson, S. J., S. Shah, M. Comiskey, Y. P. de Jong, B. Wang, E. Mizoguchu, A. K. Bhan, and C. Terhorst. 1998. T cell-mediated pathology in two models of experimental colitis depends predominantly on the interleukin 12/signal transducer and activator of transcription (Stat)-4 pathway, but is not conditional on interferon γ expression by T cells. *J. Exp. Med. 187:1225.*
36. Kennedy, M. K., K. S. Picha, W. C. Fanslow, K. H. Grabstein, M. R. Alderson, K. N. Clifford, W. A. Chin, and K. M. Mohler. 1996. CD40/CD40 ligand interactions are required for T cell-dependent production of interleukin-12 by mouse macrophages. *Eur. J. Immunol. 26:370.*
37. Koch, F., U. Stanzl, P. Jennewein, K. Janke, C. Heufler, E. Kampgen, N. Romani, and G. Schuler. 1996. High level IL-12 production by murine dendritic cells: upregulation via MHC class II and CD40 molecules and downregulation by IL-4 and IL-10. *J. Exp. Med. 184:741.*
38. Grewal, I. S., J. Xu, and R. A. Flavell. 1995. Impairment of antigen-specific T-cell priming in mice lacking CD40 in ligand. *Nature 378:617.*
39. Cong, Y., C. T. Weaver, A. Lazenby, and C. O. Elson. 2000. Colitis induced by enteric bacterial antigen-specific $CD4^+$ T cells requires CD40-CD40 ligand interactions for a sustained increase in mucosal IL-12. *J. Immunol. 165:2173.*
40. Blossom, S., E. B. Chu, W. O. Weigle, and K. M. Gilbert. 1997. CD40 ligand expressed on B cells in the BXSB mouse model of systemic lupus erythematosus. *J. Immunol. 159:4580.*
41. Yellin, M. J., K. Sippel, G. Inghirami, L. R. Covey, J. J. Lee, J. Sinning, E. A. Clark, L. Chess, and S. Lederman. 1994. CD40 molecules induce down modulation and endocytosis of T cell surface T cell-B cell activating molecule/CD40L: potential role in regulating helper effector function. *J. Immunol. 152:598.*
42. Brandtzaeg, P., and I. N. Farstad. 1999. The human mucosal B-cell system. In *Mucosal Immunology.* P. L. Ogra, J. Mestecky, M. E. Lamm, W. Strober, J. Bienenstock, and J. R. McGhee, eds. Academic Press, San Diego, p. 439.
43. Elson, C. O. 2000. The immunology of inflammatory bowel disease. In *Inflammatory Bowel Disease.* J. B. Kirsner, ed. Saunders, Philadelphia, p. 208.
44. Cicalese, L., R. H. Duerr, M. A. Nalesnik, P. F. Heeckt, K. K. Lee, and W. H. Schraut. 1995. Decreased mucosal IgA levels in ileum of patients with chronic ulcerative colitis. *Dig. Dis. Sci. 40:805.*
45. Philipsen, E. K., S. Bondesen, J. Andersen, and S. Larsen. 1995. Serum immunoglobulin G subclasses in patients with ulcerative colitis and Crohn's disease of different disease activities. *Scan. J. Gastroenterol. 30:50.*
46. Badr-el-Din, S., L. K. Trejdosiewicz, R. V. Heatley, and M. S. Losowsky. 1998. Local immunity in ulcerative colitis: evidence for defective secretory IgA production. *Gut 29:1070.*
47. Kantor, A. B., and L. A. Herzenberg. 1993. Origin of murine B cell lineages. *Annu. Rev. Immunol. 11:501.*
48. Kasaian, M. T., and P. Casali. 1993. Autoimmunity-prone B-1 (CD5 B) cells, natural antibodies and self recognition. *Autoimmunity 15:315.*
49. Mizoguchi, E., A. Mizoguchi, F. I. Preffer, and A. K. Bhan. 2000. Regulatory function of mature B cells via costimulatory pathway in a murine colitis model. *Int. Immunol. 12:597.*
50. Mizoguchi, A., E. Mizoguchi, H. Takedatsu, R. S. Blumberg, and A. K. Bhan. 2002. Chronic intestinal inflammatory condition generates IL-10-producing regulatory B cell subset characterized by CD1d upregulation. *Immunity 16:219.*

MOLECULAR AND CELLULAR BIOLOGY, July 2004, p. 6298-6310 Vol. 24, No. 14
0270-7306/04/$08.00+0 DOI: 10.1128/MCB.24.14.6298-6310.2004

Interferon Regulatory Factor 1 (IRF-1) and IRF-2 Distinctively Up-Regulate Gene Expression and Production of Interleukin-7 in Human Intestinal Epithelial Cells

Shigeru Oshima,[1]† Tetsuya Nakamura,[1]† Shin Namiki,[1] Eriko Okada,[1] Kiichiro Tsuchiya,[1] Ryuichi Okamoto,[1] Motomi Yamazaki,[1] Takanori Yokota,[2] Masatoshi Aida,[3] Yuki Yamaguchi,[3] Takanori Kanai,[1] Hiroshi Handa,[3] and Mamoru Watanabe[1]*

Department of Gastroenterology and Hepatology[1] and Department of Neurology and Neurological Sciences,[2] Graduate School, Tokyo Medical and Dental University, Bunkyo-ku, Tokyo 113-8519, and Graduate School of Bioscience and Biotechnology, Tokyo Institute of Technology, Yokohama 226-8501,[3] Japan

Received 10 September 2003/Returned for modification 16 January 2004/Accepted 19 April 2004

Intestinal epithelial cell-derived interleukin (IL)-7 functions as a pleiotropic and nonredundant cytokine in the human intestinal mucosa; however, the molecular basis of its production has remained totally unknown. We here showed that human intestinal epithelial cells both constitutively and when induced by gamma interferon (IFN-γ) produced IL-7, while several other factors we tested had no effect. Transcriptional regulation via an IFN regulatory factor element (IRF-E) on the 5′ flanking region, which lacks canonical core promoter sequences, was pivotal for both modes of IL-7 expression. IRF-1 and IRF-2, the latter of which is generally known as a transcriptional repressor, were shown to interact with IRF-E and transactivate IL-7 gene expression in an IFN-γ-inducible and constitutive manner, respectively. Indeed, tetracycline-inducible expression experiments revealed that both of these IRF proteins up-regulated IL-7 protein production, and their exclusive roles were further confirmed by small interfering RNA-mediated gene silencing systems. Moreover, these IRFs displayed distinct properties concerning the profile of IL-7 transcripts upon activation and expression patterns within human colonic epithelial tissues. These results suggest that the functional interplay between IRF-1 and IRF-2 serves as an elaborate and cooperative mechanism for timely as well as continuous regulation of IL-7 production that is essential for local immune regulation within human intestinal mucosa.

Intestinal epithelial cells (IECs) function as active participants in local immune regulation via the secretion of a variety of cytokines. Among these, interleukin-7 (IL-7) is particularly important in terms of its pleiotropic functions in the intestinal immune system. Studies have demonstrated that IEC-derived IL-7 stimulates the proliferation of lamina propria lymphocytes and intraepithelial lymphocytes (IELs) (5, 30) and also enhances cytokine release from lamina propria lymphocytes in humans (20). In addition, analyses in mice have revealed the nonredundant functions of IL-7, because inactivation of IL-7 or the IL-7 receptor gene resulted in severely impaired development of γδ-IELs, Peyer's patches, and cryptopatches, all of which play critical roles in mucosal immune regulation (13, 21, 29). These findings suggest that IL-7 production from IECs might be tightly controlled for variable levels of production that properly respond to the altered status of mucosal lymphocytes and also for the constitutive levels of secretion that might support the nonredundant functions of IL-7, for example, on the development of gut-associated lymphoid tissues. Previously, our group has demonstrated that the mRNA and protein of IL-7 are expressed throughout the epithelial layer of human colonic tissues, and the epithelial goblet cells are the type of cells where the expression of IL-7 is relatively abundant (30). To date, however, the mechanisms of IL-7 production in human IECs are poorly defined.

Lack of knowledge about the mechanism of IL-7 production is not confined to IECs but is also the case with other tissue-derived cells of human origin. Previous reports demonstrated that IL-7 production from human bone marrow (BM) stromal cells, the major cell type from which IL-7 is produced in vivo, was regulated by several cytokines such as IL-1, tumor necrosis factor alpha (TNF-α) and transforming growth factor beta (TGF-β) (27, 34); however, the intracellular mechanisms of these regulations have remained unclear. In addition, little is known about the mechanisms by which IL-7 is constitutively produced, while such cells as BM stromal cells exhibited the ability to produce a substantial amount of IL-7 even in the absence of specific cytokines in vitro (27, 34). Moreover, studies on murine tissue-derived cells rather complicated the question as to the mechanisms of IL-7 production in human cells, since these studies implied a different mechanism for murine IL-7 gene expression (3), despite a high degree of conservation in the 5′ flanking region of the IL-7 genes of both species (3, 8, 23). For example, in murine keratinocytes Pam 212 cells, ex-

* Corresponding author. Mailing address: Department of Gastroenterology and Hepatology, Graduate School, Tokyo Medical and Dental University, 1-5-45 Yushima, Bunkyo-ku, Tokyo 113-8519, Japan. Phone: 81 3 5803 5973. Fax: 81 3 5803 0262. E-mail: mamoru.gast@tmd.ac.jp.

† S.O. and T.N. contributed equally to this work.

pression of the IL-7 gene was not influenced by IL-1, TNF-α, or TGF-β but was up-regulated by another cytokine, gamma interferon (IFN-γ) (3), indicating that murine cells respond differently than human BM stromal cells to these cytokines (27, 34). These collective findings suggest that IL-7 production might be under the control of a tissue-specific and/or a species-specific regulatory mechanism. Therefore, it seems crucial to clarify the mechanisms of IL-7 production in human IECs to gain a better understanding of the functions of this cytokine on local immune regulation.

In this study, using human colonic epithelial cell lines, we showed that IL-7 protein was produced both constitutively and in response to IFN-γ in human IECs. The transcriptional regulation via an interferon regulatory factor element (IRF-E) was important for IL-7 production in human IECs, which is consistent with the previous report on murine keratinocytes. Of note, it was found that not only IRF-1 but also IRF-2, generally known as a transcriptional repressor, up-regulated IL-7 production. Intriguingly, IRF-1 and IRF-2 exclusively exerted their functions in an IFN-γ-inducible and constitutive manner, respectively, with properties to induce different sets of IL-7 transcript upon activation. Along with the demonstration that both IRF-1 and IRF-2 were expressed in normal human colonic epithelial cells, these data suggest that the functional interplay between IRF-1 and IRF-2 might serve as an elaborate mechanism for the finely tuned regulation of IL-7 production that is indispensable for local immune regulation within the human intestinal mucosa.

MATERIALS AND METHODS

Cell culture. Human colon carcinoma-derived DLD-1 and HT29-18N2 cells were maintained in Dulbecco's modified Eagle medium supplemented with 10% fetal bovine serum and 1% penicillin-streptomycin. Except where indicated otherwise, cells were seeded at a density of 3×10^5 cells/ml in the medium 36 h prior to each experiment.

ELISA. Cells at a density of 8×10^5 cells per ml of culture medium were seeded onto 24-well plates. After 36 h of culture, the medium was removed, and the cells were washed twice with phosphate-buffered saline. Following the addition of 1 ml of culture medium alone, or medium containing either human IL-1β, TNF-α, TGF-β, IFN-γ (PeproTec), or doxycycline (DOX; Clontech), cells were cultured for 24 h, and human IL-7 protein levels in the culture supernatants were measured by a human IL-7 enzyme-linked immunosorbent assay (ELISA) kit (R&D Systems).

Semiquantitative reverse transcription (RT)-PCR. Total RNA was isolated by using Trizol reagent (Invitrogen) according to the manufacturer's instructions. Aliquots of 5 μg of total RNA were used for cDNA synthesis in 21 μl of reaction volume. One microliter of cDNA was amplified with 0.25 U of LA *Taq* polymerase (TaKaRa) in a 25-μl reaction. Sense (S) and antisense (AS) primers used here were as follows: S1, 5′-AGCTTGCTCCTGCTCCAGTT-3′; S2, 5′-GAGA TCATCTGGGAAGTCTTTTACC-3′; S3, 5′-ACTTGTGGCTTCCGTGCACA CATTA-3′; AS1, 5′-TGCATTTCTCAAATGCCCTAATCCG-3′; and AS2, 5′-ATCCGCCAGCAGTGTACTTTCAGTT-3′ for human IL-7 (see Fig. 2A). For glyceraldehyde 3-phosphate dehydrogenase (G3PDH) amplification, the primers were5′-TGAAGGTCGGAGTCAACGGATTTGGT-3′ (S) and and 5′-CATGT GGGCCATGAGGTCCACCAC-3′ (AS). Each cycle of PCR amplification consisted of denaturation at 94°C for 30 sec, annealing at 61°C for 30 sec, and extension at 72°C for 30 sec. Twenty-seven cycles were performed for IL-7, and 17 cycles were performed for G3PDH, and the amplification for each gene was in the linear curve under these conditions. PCR products were separated on 1.5% agarose gels, stained by ethidium bromide, and visualized by using a Lumi-Imager F1 system (Roche).

Northern blotting. Poly(A)$^+$ mRNA was isolated by using a FastTrack 2.0 kit (Invitrogen) according to the manufacturer's instructions. Northern blotting was performed as described previously (22) by using 15 μg of poly(A)$^+$ mRNA. The cDNA probe corresponding to nucleotides at positions −55 to +681 (coding sequence [CS] probe) and −539 to −242 (5′ untranslated region [UTR] probe) for human IL-7 were generated by RT-PCR by using the primers S1/AS1 and S3/AS2, respectively, from an RNA sample of DLD-1 cells as described above. The probe for G3PDH was also generated by RT-PCR by using the primers described above. Hybridization was carried out at 42°C overnight for IL-7 and at 55°C for 2 h for G3PDH.

RLM-RACE. Determination of the transcription initiation sites of the human IL-7 gene was accomplished by RNA ligase-mediated [RLM] 5′ rapid amplification of cDNA ends [RACE] by using a GeneRacer Kit (Invitrogen). In brief, poly(A)$^+$ mRNAs extracted from IFN-γ-stimulated (6 h) DLD-1 cells were treated with calf intestinal phosphatase to eliminate 5′ phosphates from truncated mRNA without affecting 5′ capped intact mRNA. The dephosphorylated RNA was then treated with tobacco acid pyrophosphatases to remove the 5′ cap structure. The GeneRacer RNA Oligo was ligated to the 5′ end of the decapped mRNA by using T4 RNA ligase. First-strand cDNA synthesis was performed by reverse-transcribing the ligated mRNA in the presence of the GeneRacer oligo dT primer. Sequential PCRs were performed by using a primer set of the GeneRacer 5′ primer and 3′ reverse IL-7 gene-specific primer 1 (GSP-1) and then by using the nested primer set of the GeneRacer 5′ nested primer and 3′ reverse IL-7 GSP-2 to amplify only the cDNAs that have the GeneRacer RNA Oligo ligated to the 5′ end. As a control, PCR with a primer set for amplifying the 5′ part of the human β-actin gene was also performed in parallel, according to the manufacturer's recommendation. The primers used were 5′-TGCCCTA ATCCGTTTTGACCATGGTG-3′ (IL-7 GSP-1) and 5′-GCAACAGAACAAG GATCAGGGGAGG-3′ (IL-7 GSP-2). PCR products of around 600 and 300 bp were gel purified and cloned into the pGEM-T vector (Promega) independently, and then 10 clones of each were sequenced. All the clones contained the IL-7 gene sequence along with the adapter sequences, indicating these clones to be derived from mRNAs retaining complete 5′ ends.

Plasmids. The human IL-7 DNA fragment between either position −3194, −1322, −609, or −282 and −3 was amplified from human genomic DNA by PCR and ligated into the pGL3 Basic luciferase reporter plasmid (Promega) to create −3194-Luc, −1322-Luc, −609-Luc, and −282-Luc. The nucleotide position number was assigned relative to the translation start site (+1). A series of 5′ deletions of the −609-Luc, shown as −362-Luc, −251-Luc, and −215-Luc, was constructed by unidirectional digestion by using an exonuclease III. An internal deletion mutant −609-Luc-Δ-282/-251 was constructed by PCR-mediated mutagenesis. Plasmids −609-mtIRF-E-Luc and −282-mtIRF-E-Luc, both of which contain a 4-bp mutation within IRF-E, were also constructed by PCR-mediated mutagenesis. Introduced mutations and the wild-type sequences within the region of positions −280 to −253 were given with top strand sequences as follows: mutant, 5′-AAGCGCAAAGTAGAGGCTGAGGGTACAC-3′ (underlined residues indicate introduced mutations); wild type, 5′-AAGCGCAAAGTAGAAA CTGAAAGTACAC-3′. Expression vectors pcDNA3-IRF-1 and pcDNA3-IRF-2 were prepared by subcloning the PCR-amplified open reading frame of human IRF-1 and IRF-2 cDNA into a pcDNA3 (Invitrogen). To construct tetracycline (TET)-inducible expression plasmids, the open reading frames of IRF-1 and IRF-2 were subcloned into a pcDNA4/TO/Myc/His (Invitrogen) in frame. All constructs were verified by DNA sequencing.

Transient transfection and reporter assays. DLD-1 cells seeded in a 60-mm culture dish were transfected with 3 μg of reporter plasmid along with 10 ng of pRL-tk plasmid (Promega) as described previously (22). Cells were harvested 24 h after transfection, lysed by three cycles of freezing and thawing, and then luciferase activities were measured by a luminometer (Turner Designs). Luciferase activities as indicated by arbitrary unit were normalized by renilla luciferase activities in each sample.

EMSA. The preparation of nuclear extracts and electrophoretic mobility shift assays (EMSA) were performed essentially as described previously (22), except for the use of 0.5 μg of poly(dI-dC) · poly(dI-dC) per binding reaction. A DNA probe and its mutated version were prepared by annealing oligonucleotides as follows: top strand, 5′-AAGCGCAAAGTAGAAACTGAAAGT-3′, and bottom strand, 5′-GTGTACTTTCAGTTTCTACTTTG-3′, for the wild-type probe; and top strand, 5′-AAGCGCAAAGTAGAGGCTGAGGGT-3′, bottom strand, 5′-GTGTACCCTCAGCCTCTACTTTG-3′, for the mutant probe. For competition experiments, a 20-fold excess of unlabeled double-stranded probe or its mutated version was added prior to the labeled probe. In supershift experiments, antibodies (Santa Cruz Biotechnology) against either IRF-1 (catalogue no. sc-497), IRF-2 (sc-498), IRF-3 (sc-9082), IRF-4 (sc-6059), IRF-7 (sc-9083), IRF-8 (sc-6058), or IRF-9 (sc-496) were used.

Immunoblotting. Immunoblotting was performed as described elsewhere (22). Twenty-five micrograms of nuclear extracts was analyzed by using anti-IRF-1 (catalogue no. sc-497), anti-IRF-2 (sc-498), and anti-upstream factor (USF)-2 (sc-861) antibodies (all from Santa Cruz Biotechnology) at a 1:500 dilution as a

primary antibody. Proteins were visualized with an enhanced chemiluminescence detection system (Amersham Bioscience).

Establishing tetracycline-regulated IRF-1- and IRF-2-expressing DLD-1 cell lines. Sublines of DLD-1 cells, in which the expression of either IRF-1 or IRF-2 is inducible under the control of the addition of TET, were established by using a T-REx System (Invitrogen). In brief, a DLD-1-derived subclone that constitutively expresses the TET repressor (TR) was created by transfecting parental DLD-1 cells with a plasmid pcDNA6/TR (Invitrogen). Several clones were selected in the culture medium containing blasticidin (7.5 μg/ml; Invitrogen). An appropriate clone was isolated, designated as DLD-1/TR cells, and then transfected with either expression plasmid pcDNA4/TO/IRF-1-Myc/His or pcDNA4/TO/IRF-2-Myc/His. Cells stably expressing each of these genes were selected in the presence of 750 μg of Zeocin (Invitrogen) per ml to establish the sublines designated as DLD-1/TR/IRF-1-tag or DLD-1/TR/IRF-2-tag cells. In all experiments, we used DOX as an alternative inducer of gene expression because it has a longer half-life than TET.

siRNA experiments. All small interfering RNA (siRNA) duplex oligonucleotides were synthesized and subsequently annealed for use. DLD-1 cells were seeded at a density of 3×10^5 cells per ml onto a 24-well plate or a 100-mm culture dish. After 36 h, cells were transfected with 100 nM siRNA oligonucleotides as described previously (37), and the siRNA-containing medium was removed after 12 h of transfection. Cells were cultured for an additional 12 h under the usual conditions, and then the medium was exchanged with either the medium alone or medium containing IFN-γ. For immunoblotting analysis, cells were collected from the 100-mm dishes after 12 h of medium exchange, and the nuclear extracts were isolated. For the ELISA, the culture supernatants were collected from the 24-well plates after 24 h of medium exchange. The sequences of siRNAs used here were as follows (S strand only): IRF-1, CCAAGAACCA GAGAAAAGA*TT*; IRF-2, CUCUUUAGAAACUGGGCAA*TT*; and negative control (G85R mutant superoxide dismutase), UGUUGGAGACUUCGGCAA U*TT*. Italicized letters indicate deoxynucleotides.

ChIP assays. A chromatin immunoprecipitation (ChIP) assay was performed essentially as described previously (24) with some modifications. DLD-1 cells seeded onto a 150-mm dish were stimulated with IFN-γ or left untreated for 6 h, cross-linked with 1% formaldehyde for 5 min at room temperature, and then quenched by adding glycine. Cells were washed with phosphate-buffered saline, resuspended in 1 ml of lysis buffer (10 mM Tris-HCl [pH 8.0], 0.25% Triton X-100, 10 mM EDTA, and 0.5 mM EGTA) and left on ice for 10 min. After centrifugation, the nuclei were washed with 1 ml of wash buffer (10 mM Tris-HCl [pH 8.0], 200 mM NaCl, 10 mM EDTA, and 0.5 mM EGTA, 10 mM sodium butyrate, 20 mM β-glycerophosphate, 100 μM sodium orthovanadate, 1 μM microcystin, and the protease inhibitor cocktail) and resuspended in 400 μl of sonication buffer (10 mM Tris-HCl [pH 8.0], 100 mM NaCl, 1 mM EDTA, and 0.5 mM EGTA). The sonication was performed in two steps by using a VP-152 system (TAITEC); the first step was carried out for 5 min, followed by the addition of 50 μl of 10% sodium dodecyl sulfate (SDS) and incubation for 1 h to solubilize the chromatin, and then the second sonication was performed for 4 min. This yielded genomic fragments with an average size of 500 bp. Aliquots (100-μl) of sheared chromatin were diluted into 1 ml of radioimmunoprecipitation assay (RIPA) buffer (10 mM Tris-HCl [pH 8.0], 1% Triton X-100, 0.1% SDS, 0.1% sodium deoxycholate, 1 mM EDTA, 0.5 mM EGTA, and 140 mM NaCl) and precleared with 50 μl of protein G-Sepharose (50% slurry in RIPA buffer) for 1 h at 4°C. Immunoprecipitation was performed overnight at 4°C with 10 μg of an anti-IRF-1 (catalogue no. sc-497), anti-IRF-2 (sc-498), normal mouse immunoglobulin G (IgG; sc-2025) (all from Santa Cruz Biotechnology), or an antihistone H3 antibody (Abcam, Inc.). A 20-μl aliquot of 50% protein G-Sepharose slurry (same as above but containing 2 mg of herring sperm DNA per ml and 2 mg of bovine serum albumin per ml) was added to each and incubated for 1 h at 4°C. Precipitates were washed sequentially in RIPA buffer three times, in 0.5 M NaCl RIPA buffer (same as RIPA buffer but with 500 mM NaCl) three times, in LiCl wash buffer (10 mM Tris-HCl [pH 8.0], 0.25 M LiCl, 1% NP-40, 1% sodium deoxycholate, 1 mM EDTA, 1 mM EGTA, 10 mM sodium butyrate, 100 μM sodium orthovanadate, and the protease inhibitor cocktail) twice, and in TE buffer (10 mM Tris-HCl [pH 8.0], 1 mM EDTA) twice, for 3 min for each wash. Samples were extracted twice with 50 μl of elution buffer (1% SDS, 0.1 M NaHCO3, 10 mM dithiothreitol) and digested with 2 μg of proteinase K at 37°C for 4 h. Then 4 μl of 5 M NaCl was added, and the samples were incubated at 65°C overnight to reverse cross-linking. DNA fragments were recovered by phenol-chloroform extraction and ethanol precipitation.

The genomic DNA fragments in the immunoprecipitated samples were analyzed by PCR by using a primer set for amplifying the −539 to −159 region of the human IL-7 gene (5′-ACTTGTGGCTTCCGTGCACACATTA-3′ and 5′-G ACTGCAGTTTCATCCATCCCAAG-3′) to detect the IRF-E-containing fragment, and another set for the +976 to +1337 region (5′-GCTCTTTCTTTT GATGGCTACTCCG-3′ and 5′-TAGCCCATGATTCATATAACTGTGC-3′; numbers indicate the positions on the genomic DNA relative to the translation start site) (see Fig. 8A) as controls. Initially, quantitative PCR on a LightCycler system (Roche) was performed to quantify the immunoprecipitated DNA. A 5-μl aliquot from a total of 100 μl of DNA solution was amplified and the threshold cycle was obtained from each amplification curve. In practice, DNA fragments were nonspecifically and reproducibly recovered after the ChIP assay in the absence of specific antibody but were usually amplified 5 to 6 cycles later than specifically recovered fragments. By using software provided by the manufacturer, the amount of DNA fragment in each sample was calculated relative to the standard curve obtained by the three different dilutions of input DNAs (10, 1, and 0.1%). Three independent chromatin preparations were made, and the average value obtained for each sample was indicated as a percentage of total input DNA. The same amounts of DNA samples or the diluted inputs were also analyzed by conventional PCR in parallel with the following parameters: denaturation at 94°C for 15 s, annealing at 61°C for 30 s, and extension at 72°C for 30 s for 37 cycles. The products were resolved by agarose gel electrophoresis, stained with ethidium bromide, and visualized by using a Lumi-Imager F1 system (Roche).

Immunohistochemistry. Normal colonic mucosae were obtained from three patients with colorectal cancer who underwent colectomy. Written informed consent was obtained from all patients, and these experiments were approved by the Tokyo Medical and Dental University Hospital Committee on Human Subjects. Samples fixed by 4% paraformaldehyde were cut into 8 μm-thick sections, treated with 0.5% hydrogen peroxide in methanol solution, blocked for 45 min, and then incubated with either an anti-IRF-1 (catalogue no. sc-497; Santa Cruz Biotechnology), an anti-IRF-2 (sc-13042), or purified rabbit IgG (10 mg/ml; negative control) overnight at 4°C. The sections were incubated with biotinylated goat antirabbit IgG for 60 min and reacted with streptavidin-enzyme conjugates (Vector Laboratories Inc), and then the peroxidase activities were developed by diaminobenzidin. After the samples were counterstained with hematoxylin, the localization of IRF-1 or IRF-2 was examined by light microscopy.

RESULTS

Human IECs constitutively produce IL-7, and IL-1, TNF-α, and TGF-β have no influence on the levels of IL-7 production, but IFN-γ does. To investigate the mechanisms of IL-7 production in human IECs, human colonic epithelial cell lines, DLD-1 and HT29-18N2 cells, were analyzed. Previous reports showed that both IL-1 and TNF-α had enhancing effects on IL-7 production in human BM stromal cells or osteoblasts (34), while TGF-β had suppressive effects on IL-7 production in BM stromal cells (27). In contrast, shown with murine keratinocytes, none of these cytokines had any effect, while IFN-γ solely exhibited enhancing effects on IL-7 mRNA expression among various factors (3). Therefore, to test whether IL-7 production in human IECs is also diversely regulated by these cytokines, DLD-1 and HT29-18N2 cells were incubated for 24 h with either IL-1, TNF-α, TGF-β, IFN-γ, or the medium alone, and IL-7 production was measured by ELISA. As shown in Fig. 1, both of these cells constitutively produced substantial amounts of IL-7 protein, with a higher concentration per cell number in DLD-1 than in HT29-18N2 cells. In addition, treatment with IFN-γ significantly enhanced IL-7 production in both cell types, while stimulation with IL-1, TNF-α, or TGF-β had no effect (Fig. 1). We also tested the possibility that TGF-β might act as an inhibitory factor not for the constitutive but for the inducible production of IL-7, but treatment with TGF-β did not affect IFN-γ-inducible IL-7 production (Fig. 1). These data indicated that human IECs produce IL-7 both constitutively and in response to IFN-γ, while several other cytokines have no regulatory effect on this process.

Transcription start sites of the human IL-7 gene are clustered within two distinct regions, and IFN-γ preferentially

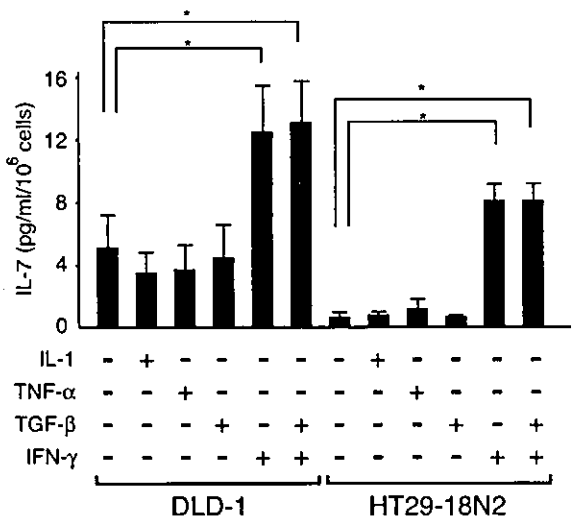

FIG. 1. Human IECs constitutively produce IL-7, and IL-1, TNF-α, and TGF-β do not influence the levels of IL-7 production, whereas IFN-γ does. DLD-1 and HT29-18N2 cells were cultured in medium alone or in medium containing 50 ng of either IL-1, TNF-α, TGF-β, IFN-γ, or IFN-γ plus TGF-β per ml for 24 h. The supernatants were collected and assayed for IL-7 production by ELISA. Results are the means ± standard deviations of three independent experiments. *, $P < 0.05$ by a paired Student t test.

induces short species of mRNA via a selective usage of downstream initiation sites. Human tissues have been shown to express two major IL-7 mRNAs of ~1.8 and ~2.4 kb, and this has been inferred as a result of alternative polyadenylation (8). To examine whether constitutive and IFN-γ-inducible IL-7 protein production is regulated at the mRNA level, we next assessed the expression of IL-7 transcripts by Northern blot analysis by using a cDNA probe covering the IL-7 protein coding sequences (Fig. 2A, CS probe). In DLD-1 cells, two major mRNA species were clearly observed in the absence of IFN-γ (Fig. 2B, left). Since each of these bands migrated somewhat heterogeneously, it was difficult to determine the precise size of these transcripts. However, the analysis of mRNAs extracted from SK-Hep1 cells, human hepatocellular carcinoma cells originally used for the cloning of the human IL-7 gene (8), showed equally migrating bands (data not shown). Thus, we tentatively equated these transcripts with those described previously (8). When DLD-1 cells were treated with IFN-γ, ~1.8-kb mRNA was significantly induced within 6 h, whereas the increase in ~2.4-kb mRNA was modest (Fig. 2B, left). Although the basal level of IL-7 mRNA was lower in HT29-18N2 cells than could be visualized, these cells displayed a similar pattern of IL-7 mRNA expression: IFN-γ significantly induced expression of ~1.8-kb and, to a lesser extent, ~2.4-kb of mRNAs (Fig. 2B, right). These data indicated that the levels of IL-7 protein production correlate well with those of mRNA expression and that IFN-γ treatment predominantly induces the short mRNA species of the IL-7 gene. Interestingly, in murine keratinocytes, IFN-γ treatment was demonstrated to induce the expression of relatively short species of IL-7 mRNA through the use of alternative transcription start sites (3). Given an analogy in IFN-γ-dependent induction of selective IL-7 transcripts between human IECs and murine keratinocytes, it seemed possible that the mechanisms of IFN-γ-dependent IL-7 gene expression are, at least in part, conserved between these two cell types.

To date, a detailed analysis of the transcription start sites for the human IL-7 gene has not been reported. We thus at-

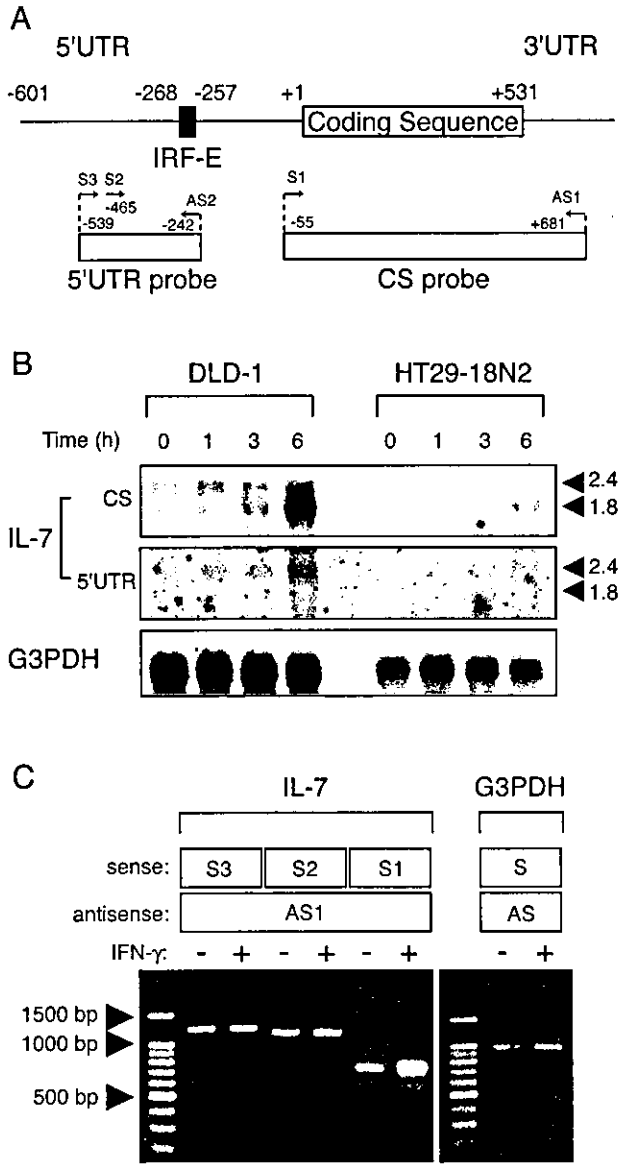

FIG. 2. IFN-γ-dependent and -independent IL-7 production is distinctively regulated by expression of IL-7 transcripts that differ in their 5′ UTR. (A) Schematic drawing of human IL-7 mRNA, with the primers and cDNA probes used in this study. The nucleotide number was designated with respect to the translation start site (+1). An IRF-E located at the region from position −268 to −257 is also indicated. (B) DLD-1 and HT29-18N2 cells were stimulated with IFN-γ (50 ng/ml) for the indicated time periods. Fifteen micrograms of poly(A)$^+$ mRNA was subjected to Northern blotting for IL-7 mRNA by using the ^{32}P-labeled CS probe or the 5′ UTR probe. The bottom panel indicates the level of G3PDH mRNA as a control. (C) DLD-1 cells were treated with IFN-γ (50 ng/ml) or left untreated for 6 h, collected for total RNA isolation, and then subjected to semiquantitative RT-PCR for IL-7 mRNA. PCR amplification was performed by using either the S1, S2, or S3 primer along with AS1 primer depicted in panel A. As controls, samples from IFN-γ-treated and untreated cells were amplified with a primer set for G3PDH.

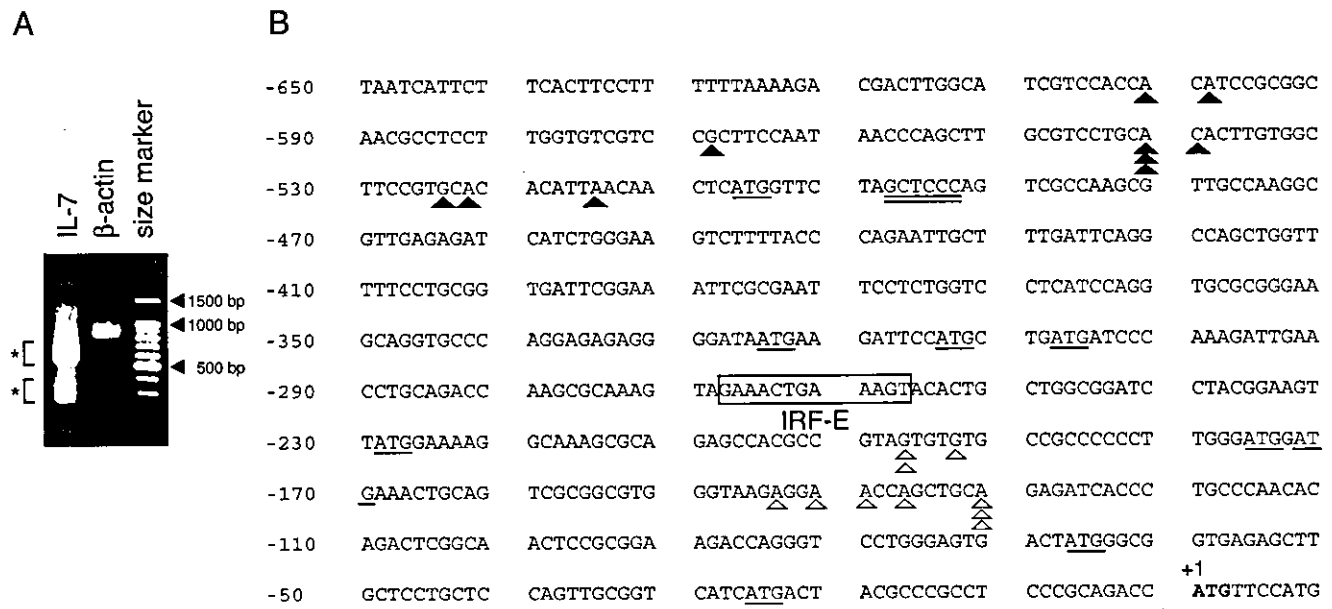

FIG. 3. Transcription initiation sites for the human IL-7 gene were clustered within two separate regions upstream from the translation start site. (A) RLM-RACE analysis was performed by using poly(A)$^+$ RNAs from IFN-γ-treated (6 h) DLD-1 cells as described in Materials and Methods. PCR products amplified by a primer set for the IL-7 or β-actin gene, respectively, were run on 1.5% agarose gel, stained with ethidium bromide, and visualized. (B) Two major fragments of ~600 and ~300 bp shown in panel A were independently cloned, and then 10 clones of each were sequenced. The 5′ end of each clone is shown by a filled triangle (clones derived from ~600-bp fragments) or an open triangle (clones from ~300-bp fragments) on the first 650 bp of sequence upstream of the translation start site. The authentic translation start site is indicated in bold. Numbering in base pairs is indicated to the left, with negative numbers representing nucleotides upstream of the ATG. Consensus sequences for the IRF-E are boxed and labeled. Potential translation initiation codons (ATG) are underlined. Consensus sequences for MED-1 are also underlined.

tempted to precisely map the 5′ end of IL-7 mRNA by using a RLM-RACE method that ensures the amplification of only full-length transcripts via the elimination of truncated mRNAs (see Materials and Methods). When poly(A)$^+$ RNA extracted from IFN-γ-treated (6 h) DLD-1 cells was analyzed, fragments around 600 and 300 bp were obtained by PCR by using the 5′ nested primer and the 3′ reverse IL-7 GSP-2 (corresponding to nucleotides 36 to 60 of the IL-7 gene) (Fig. 3A). No product was obtained when RNA was not treated with tobacco acid pyrophosphatases, indicating that these products were derived from full-length mRNA (data not shown). Both of these products appeared to migrate somewhat diffusely when subjected to gel electrophoresis (Fig. 3A). This result was not attributable to experimental artifacts, because PCR amplification with another set of primers, designed for detecting the 5′ part of the human β-actin gene, yielded products of the expected size (872 bp) that migrated as a single band from the same sample (Fig. 3A). The ~600- and ~300-bp fragments were independently isolated and cloned, and then 10 clones of each were sequenced. All 20 clones contained the IL-7 gene sequence along with the adapter sequences, showing these clones to be derived from mRNAs retaining complete 5′ ends. Alternative splicing appeared to be infrequent in this region (upstream of the sequences corresponding to IL-7 GSP-2), because no nucleotide deletion was observed in any of the sequenced clones. As depicted in Fig. 3B, the 5′ ends of longer fragments were located within the −601 to −515 region upstream of the translation start site (+1), while the 5′ ends of shorter fragments were mapped within the −197 to −131 region. These results demonstrated that the human IL-7 gene is transcribed from multiple transcription start sites that are clustered within two distinct regions approximately 300 to 500 bp apart from each other.

We then tested whether ~1.8- and ~2.4-kb IL-7 mRNAs might indeed differ in their 5′ UTR stretches by Northern blot analysis using a 5′ UTR probe corresponding to nucleotides at positions −539 to −242 (Fig. 2A). Interestingly, this probe exhibited subtle but substantial hybridization with ~2.4-kb but not with ~1.8-kb mRNA, showing the different lengths of 5′ UTR between these mRNA species (Fig. 2B). To further confirm this, RT-PCR with any of the S primers (S1, S2, or S3) along with the AS1 primer (Fig. 2A) was carried out. When RNAs from untreated and IFN-γ-treated DLD-1 cells were examined, amplification with the primer sets of S3/AS1 and S2/AS1 showed no difference in the amount of products before and after IFN-γ treatment (Fig. 2C). In contrast, amplification with the primer set of S1/AS1 displayed a significant increase in the amounts of PCR products in response to IFN-γ (Fig. 2C). Therefore, it was demonstrated that stimulation with IFN-γ preferentially induces relatively short-form IL-7 mRNA expression via the selective usage of transcription initiation sites within the region −197 to −131. Of note, the maximum difference in 5′ UTR lengths among clones obtained in RLM-RACE was less than 500 bp and did not match that between the ~2.4- and ~1.8-kb transcripts seen in Northern blot analysis. We assumed that this discrepancy might have in some part resulted from the difficulties in determining the precise size of transcripts by Northern blot analysis; however, this issue was not further examined in the present study.